Journal of the Geological Society

New structural and Re-Os geochronological evidence constraining the age of faulting and associated mineralization in the Devonian Orcadian Basin, Scotland

--Manuscript Draft--

Manuscript Number:	jgs2015-118R1
Article Type:	Research article
Full Title:	New structural and Re-Os geochronological evidence constraining the age of faulting and associated mineralization in the Devonian Orcadian Basin, Scotland
Short Title:	Age of faulting and mineralization in the Orcadian Basin
Corresponding Author:	Robert Edmund Holdsworth, PhD Durham University Durham, UNITED KINGDOM
Corresponding Author E-Mail:	r.e.holdsworth@durham.ac.uk
Other Authors:	Anna Dichiarante
	Edward Dempsey
	David Selby
	Ken McCaffrey
	Uisdean Michie
	Graeme Morgan
	Jason Bonniface
Abstract:	The Devonian Orcadian Basin in northern Scotland belongs to a regionally linked system of post-Caledonian continental basins extending northwards to western Norway and eastern Greenland. Extensional fault systems that cut the Orcadian Basin sequences are commonly assumed to be Devonian, with some limited inversion and reactivation proposed during the Carboniferous and later times. We present a detailed structural study of the regionally recognized fault systems exposed in the Dounreay area of Caithness which host significant amounts of authigenic mineralization (carbonate, base metal sulphides, bitumen). Structural and microstructural analyses combined with Re-Os geochronology have been used to date syn-deformational fault infills (pyrite) suggesting that faulting, brecciation and fluid flow events are likely to have occurred during the Permian (267.5 ± 3.4 [3.5] Ma). Stress inversion of fault slickenline data associated with mineralization suggest NW-SE regional rifting, an episode also recognized farther west in Sutherland. Thus a dominant set of Permian age brittle faults is now recognized along the entire north coast of Scotland forming part of the regional-scale North Coast Transfer Zone located on the southern margin of the offshore West Orkney Basin.
Manuscript Classifications:	Dating (radiometric, absolute, etc); Petroleum geology; Structural geology
Additional Information:	
Question	**Response**
Are there any conflicting interests, financial or otherwise?	No
Samples used for data or illustrations in this article have been collected in a responsible manner	Confirmed
Response to Reviewers:	See attached file

New structural and Re-Os geochronological evidence constraining the age of faulting and associated mineralization in the Devonian Orcadian Basin, Scotland

A.M. DICHIARANTE[a], R.E. HOLDSWORTH[a], E.D. DEMPSEY[a], D. SELBY[a], K.J.W.McCAFFREY[a], U. McL. MICHIE[b§], G. MORGAN[c], J. BONNIFACE[c]
a = Department of Earth Sciences, Durham University, Durham DH1 3LE, UK
b = Vine Lodge, Vine Road, Johnston, Haverfordwest, SA62 3NZ, UK.
c = *Dounreay Site Restoration Limited, Dounreay, Caithness, KW14 7TZ, UK*
§ = deceased 20th June 2015

Abstract: The Devonian Orcadian Basin in northern Scotland belongs to a regionally linked system of post-Caledonian continental basins extending northwards to western Norway and eastern Greenland. Extensional fault systems that cut the Orcadian Basin sequences are commonly assumed to be Devonian, with some limited inversion and reactivation proposed during the Carboniferous and later times. We present a detailed structural study of the regionally recognized fault systems exposed in the Dounreay area of Caithness which host significant amounts of authigenic mineralization (carbonate, base metal sulphides, bitumen). Structural and microstructural analyses combined with Re-Os geochronology have been used to date syn-deformational fault infills (pyrite) suggesting that faulting, brecciation and fluid flow events are likely to have occurred during the Permian (267.5 ± 3.4 [3.5] Ma). Stress inversion of fault slickenline data associated with mineralization suggest NW-SE regional rifting, an episode also recognized farther west in Sutherland. Thus a dominant set of Permian age brittle faults is now recognized along the entire north coast of Scotland forming part of the regional-scale North Coast Transfer Zone located on the southern margin of the offshore West Orkney Basin.

Keywords: faulting, mineralization, West Orkney Basin, Orcadian Basin, Re-Os

geochronology, Dounreay

Supplementary Material: Onshore and offshore fault/fracture lineament data are available at http://www.geolsoc.org.uk/xxxxxx.

1. Introduction

It has long been recognized that individual regional faulting episodes are often associated with characteristic fault rocks and/or mineral vein fillings (e.g. Sibson 1977; Passchier & Trouw 2005). It is usually easy to establish the relative ages of different fault rocks and vein fills based on cross cutting relationships observed both in the field and thin section (e.g. see Imber *et al.* 2001; Dempsey *et al.* 2014). The absolute dating of fault movements based on geochronological dating of fault rocks or newly-formed syn-tectonic minerals has proved to be rather more problematical. This is due to both a lack of sufficiently robust isotopic systems and suitable geological materials, especially in upper crustal settings (e.g. see van der Pluijm *et al*. 2001 and references therein).

Absolute ages of both base metal sulphide mineralization (e.g., molybdenite, pyrite, chalcopyrite) and hydrocarbon maturation (oil, bitumen) can be determined by Re-Os geochronology (e.g. Stein *et al*., 2001; Morelli *et al.,* 2004; Selby *et al*., 2009; Finlay *et al*., 2011, Finlay *et al.,* 2012) in a wide variety of crustal and tectonic settings. Both base metal sulphides and hydrocarbons are widely found associated with upper crustal faulting episodes in sedimentary basins and basement terrains worldwide. Provided there is field and microstructural evidence to show that dated fault rocks or vein fills are syn-tectonic with respect to faulting, this allows dating of the mineral fills to also be used to constrain the absolute timing of brittle deformation events (e.g. Vernon *et al*. 2014;

Holdsworth *et al.* 2015).

In this paper, we present a structural geological analysis of faults, fractures and minor folds developed in Middle Devonian rocks of the Orcadian Basin (Fig. 1) in the Dounreay region between Sandside and Crosskirk bays on the north coast of Scotland (Fig. 2a). The dominant NNE-SSW-trending brittle faults are closely associated with syn-tectonic carbonate-sulphide-hydrocarbon (bitumen) mineralization. We use Re-Os geochronology to ascertain the absolute age of the mineralization and therefore the timing of this regionally recognized episode of faulting. *In-situ* kinematic indicators from the faults are then employed to carry out stress inversion analyses to assess the style of tectonism and direction of regional extension. We show that the age of mineralization and faulting is significantly younger than has hitherto been assumed and then examine the implications of our findings for the understanding of Late Palaeozoic to Mesozoic tectonics in this part of Scotland.

2. Regional Geological Setting

2.1 Orcadian basin

The Devonian Orcadian Basin occurs onshore and offshore in the Caithness, Orkney and the Moray Firth regions of northern Scotland, overlying Caledonian basement rocks of the Northern (Moine) and Central Highland (Dalradian) terranes (Fig. 1; Johnstone & Mykura 1989; Friend *et al.* 2000). The Orcadian Basin belongs to a regionally linked system of Devonian basins that extend northwards into Shetland, western Norway and eastern Greenland (Fig. 1; Serrane 1992; Duncan & Buxton 1995, Woodcock & Strachan 2002). It is partially overlain by a number of Permian to Cenozoic, mainly offshore basins, including the West Orkney and Moray Firth basins (Fig. 1).

Lower Devonian (Emsian) syn-rift alluvial fan and fluvial-lacustrine deposits are mostly restricted to the western part of the Moray Firth region (Rogers *et al.* 1989) and parts of Caithness (NIREX 1994a) occurring in a number of small fault-bounded basins of limited extent. These are partially unconformably overlain by Middle Devonian (Eifelian-Givetian) syn-rift alluvial, fluvial, lacustrine and locally marine sequences that dominate the onshore sequences exposed in Caithness, Orkney and Shetland (Fig. 2, Marshall & Hewitt 2003). These are overlain by Upper Devonian (latest Givetian-Famennian) post-rift fluvial and marginal aeolian sedimentary rocks (Friend *et al.* 2000). In Caithness, these younger rocks are only found in a fault-bounded outlier at Dunnet Head (Fig. 1).

2.2 Basin formation

The origin of the Orcadian and nearby West Orkney basins have been a matter of some debate. Interpretations of deep crustal and shallow commercial seismic reflection profiles north of Scotland suggested that the West Orkney Basin comprises a series of half grabens bounded by easterly dipping normal faults (e.g. Brewer & Smythe 1984; Coward & Enfield 1987). Earlier interpretations (e.g. McClay *et al.* 1986; Enfield & Coward 1987; Norton *et al.* 1987) suggested that much of the basin fill was Devonian and that both the Orcadian and West Orkney basins formed due to the extensional collapse of the Caledonian orogeny. In these models, the graben-bounding faults were interpreted to root downwards into extensionally reactivated Caledonian thrusts. More recent studies have cast doubt on these models, showing that the fill of the West Orkney Basin is predominantly Permo-Triassic (e.g. Stoker *et al.* 1993) and that there is only limited onshore evidence for basement reactivation (e.g. Roberts & Holdsworth 1999; Wilson *et al.* 2010). Rifting in N Scotland during the Devonian is now considered to be related to regional sinistral transtension during left-lateral shear along the Great Glen-Walls Boundary Fault system (Seranne 1992; Dewey & Strachan 2003; Watts *et al.* 2007); the dominant rift controlling faults at this time trend generally N-S and facilitate E-W extension (see Wilson *et al.* 2010). The extent of post-Carboniferous faulting and extension onshore in Scotland is uncertain, but it could be significant (Roberts & Holdsworth 1999).

The Devonian rocks in the onshore Orcadian Basin are cut by numerous sets of faults and fractures and, more locally, are also folded (e.g. Enfield & Coward 1987; Norton *et al.* 1987; Coward *et al.* 1989; Fletcher & Key 1992; NIREX 1994a, b). Most authors have assumed that the structures are either Devonian and are rift-related and/or that they are a result of later Permo-Carboniferous basin inversion possibly related to the far-field effects of the Variscan orogenic event and/or to dextral strike-slip reactivation of the Great Glen Fault (e.g. Coward *et al*. 1989; Serrane 1992). The present paper is the first attempt at providing direct evidence to constrain the absolute ages of faulting in the Orcadian basin.

A regional study along the northern coastline of Scotland in the basement dominated region lying to the west of the Orcadian Basin presented field evidence that faults hosted in basement rocks and overlying Devonian and Permo-Triassic red bed outliers are the result of two kinematically distinct phases of rifting (Wilson *et al.* 2010). These authors documented an early phase of ENE-WSW extension related to Devonian sinistral transtension associated with the Great Glen Fault movements (Dewey & Strachan 2003) that was overprinted by a widely developed later phase of NW-SE extension. Geological and palaeomagnetic evidence from fault rocks and red bed sedimentary rocks in the Tongue and Durness regions (Blumstein *et al*. 2005; Wilson *et al.* 2010; Elmore *et al.* 2010) suggest that this later rifting was Permo-Triassic and related to the offshore development of the West Orkney and Minch basins. This raises the intriguing possibility that some of the faulting in the onshore Orcadian Basin may also be Permian or younger.

3. The Geology of the Dounreay area

The Dounreay district (Fig. 2) was extensively remapped and geophysically surveyed as part of the investigations by Nirex into the possible siting of disposal facilities for intermediate-level radioactive waste close to the site of the soon to be decommissioned nuclear power station (e.g. Fletcher & Key 1992; Nirex 1994a, b). Further detailed surveying (including surface mapping, drilling of shallow boreholes, geophysical surveys and shallow trenching) was carried out during the last decade around the Dounreay nuclear research establishment to inform the construction of sub-surface disposal facilities for low level radioactive waste (LLW). These investigations led to a series of reports concerning the geological, hydrogeological and geotechnical aspects of the site (e.g. Michie & Bonniface 2009 and references therein).

The Dounreay district lies in the western part of the onshore outcrop of the

Orcadian Basin and comprises predominantly lacustrine rhythmically-bedded Middle Devonian (Eifelian) sandstones, siltstones and shales (British Geological Survey 1985, 2005; Fletcher & Key 1992; Nirex 1994a). These rocks – part of the Caithness Flagstone Group - overlie a pre-Devonian crystalline basement of Precambrian Moine rocks intruded by the Reay Diorite, part of the ca. 426 Ma Strath Halladale Granite Complex (Fig. 2; Fletcher & Key 1992; Kocks *et al.* 2006).

The shallowly NW-dipping surface exposures of the Caithness Flagstone Group are conveniently sub-divided into four formations that are collectively estimated to form a succession over 1 km thick: (oldest to youngest) the Bighouse, Sandside Bay, Dounreay Shore and Crosskirk Bay formations (British Geological Survey 2005). Detailed stratigraphical correlations were made from surface exposures, together with the results of core and wireline logging of the successions penetrated by two Nirex deep boreholes (BH1, BH2, Fig. 2; Nirex 1994c). The boreholes intersected the crystalline basement at ca. 375m (BH1) and 560m (BH2) depth, with BH2 also cutting through an intervening ca. 100m thick basal sequence of siltstones, mudstones, sandstones and conglomerates inferred to be Lower Devonian (Emsian; British Geological Survey 2005) (Fig. 2). Detailed descriptions of the lithologies and fault structures found in the Dounreay district are reported in Fletcher & Key (1992).

Here we present a new surface lineament analysis, together with a general field description of the main brittle faults and fractures in the area. Structures preserved in coastal sections and in recent excavations for the LLW disposal facilities sited near to the Dounreay nuclear research establishment are examined in detail in order to determine the geological and microstructural relationships between faulting and carbonate-pyrite-hydrocarbon mineralization. Fresh samples of sulphide mineralization discovered along faults in the LLW excavations have then been dated using the Re-Os pyrite geochronometer.

3.1 Lineament analysis

An onshore and (near) offshore lineament analysis was conducted using satellite images and high-resolution bathymetric data, respectively. Both the onshore lineament analysis and fieldwork were largely restricted to the coast because of the flat topography of Caithness and the thick soil and glacial till limiting exposure inland. Published geological maps and field observations were used to ensure that the picked lineaments correspond to faults, fractures and joints. This also helped to create a "hierarchy" of structures which could help in the analysis of fault patterns and structural evolution of the area.

Spatial and statistical analyses were performed using ArcGis10, GEOrient and Google Earth Landsat images. 1372 lineaments were recognized at 1:2000 scale and are interpreted to be small-scale faults and joints (Fig. 3a). The trends of 102 lineaments picked on bathymetric maps were also recorded (Fig. 3b) together with 53 faults reported on existing geological maps (Fig. 3c; British Geological Survey 2005) enabling the inference of fault patterns at different scales.

The onshore lineament analysis (Fig.3a) revealed two dominant sets of structures: NE-SW to ENE-SW (40° scatter) and WNW-ESE (20° scatter) with a statistical mean trending 076° (red arrow in Fig. 3a *left*). Relative length distribution plots (Fig. 3a *right*) show that WNW lineaments are typically 3 to 4 times shorter than the NE to ENE lineaments. However, the longest onshore lineaments in the area (>300m) are N to NNE and NE trending. Up to four major sets of lineaments are well developed in the bathymetric map (Fig.3b left): N-S to NNE-SSW (30° scatter), E-W (20° scatter), NW and NE with statistical mean trending 020° (red arrow in Fig. 3b right). Relative length distribution plots (Fig. 3b) show that E-W and NW-SE lineaments are normally 4 times shorter than the N-S and NE-SW lineaments. Faults examined on existing maps (Fig. 3c) are generally N-S to NNE-SSW and NE-SW trending with the longer lineaments (>8km) trending 020° (Fig. 2, 3c right). Many faults form deep sub-vertical gully features on the coastline known locally as "geos".

When viewed as a single data set (Fig. 3d), the onshore-offshore lineaments show that the longest features correspond to the major faults shown on published maps of the area that trend N-S to NNE-SSW. The abundant NE-SW and NW-SE structures are much shorter features and appear to correspond to subordinate sets of faults and joints. This interpretation is consistent with the detailed analysis of regional fault and jointing patterns presented by Fletcher & Key (1992).

3.2 Field and microstructural observations

3.2.1 Major structures

From Sandside Bay to Brims Ness the general trend of the coast is NE-SW (Fig. 2). The bedding of the Caithness Flagstone Group dips between 5° to 12° NNW to NW (Figs 2, 4g, 5a). Local variations in strike appear to be related to rotations of bedding adjacent to some of the larger mapped faults. A densely faulted section lies in the region between the Dog Track and Gie Uisg Geo faults (Figs 2, 5a). In this section, the bedding strikes are locally rotated anticlockwise up to 35°, a change reflected by a subtle change in the orientation of the coastline in this area (Fig. 2). The cliff line here is interrupted by several vertical geos which are produced by selective erosion along weaknesses in the rocks caused by fracturing and faulting (Figs 4a, 5c). Their orientation is mainly to NNE-SSE, although subordinate numbers of NE-SW and NW-SE trends occur locally in the southern part of the coastal section.

The rocks studied here represent the western footwall of the unexposed NNE-SSW trending Bridge of Forss Fault Zone (Fig. 2). Due to a lack of well-defined fossil fish-bearing horizons in this part of Caithness, significant difficulties exist in precisely correlating the Middle Devonian sequences either side of this major fault zone. Thus the magnitude of movement along the Bridge of Forss Fault is unknown, but it is likely to be at least several hundred metres. It is suggested that this structure has significant syn-depositional SE-side down movements and that it separates the basin margin sequence to the NW from a thicker basin sequence to the SE, with numerous phases of subsequent reactivation also proposed (e.g. Fletcher & Key 1992; Nirex 1994a, b).

The other major structures are the branching NNE-SSW trending Sandside Bay, Ling Geo and Dog Track faults (Fig. 2). Based on stratigraphical offsets, throws of 75-120 m have been estimated for the Sandside Bay and Ling Geo faults (Fletcher & Key 1992). The Dog Track Fault has a more complex curved geometry swinging from a NNW trend inland to a NNE trend at the coast, branching into several fault strands including the Gling Glang, Gully-Horsetail and Geodh nam Fitheach Faults (Figs 2, 5c). The Dog Track Fault dips steeply to the SE and the offsets of the stratigraphical succession suggest a SE-side down sense of offset of at least 125 m where this fault is intersected by the Nirex BH2 borehole (Fig. 2; Michie & Bonniface 2009). As the fault branches to the north, displacement is progressively transferred from the Dog Track Fault onto the Geodh nam Fitheach Fault which shows 65 m of SE-side down offset close to the LLW facilities (Fig. 5a; Michie & Bonniface 2009).

3.2.2 Minor structures in coastal exposures

The accessible parts of the cliffs and rock platform were studied in the region between the Dog Track and Geodh nam Fhitheach faults (Figs 4a-g, 5a). Two main sets of faults and fractures are recognized trending NNE and NW. The dominant NNE-SSW trending faults show moderate to steep WNW or ESE dips (Fig. 4g). Where slickenlines are exposed on fault planes, they consistently show dextral oblique extensional kinematics (Figs 4b, c). The strata in the immediate vicinity of these structures are largely undeformed, apart from occasional tilting, most likely due to transfer of displacement between linked faults in an array (Fig. 4e). Most faults exhibit narrow (<10 cm wide) zones of brecciation often cemented by pale carbonate mineralization (Fig. 4c). Locally, thicker lenses of breccia up to a few tens of cm wide are associated with fault bends and relay zones (e.g. Fig. 4b). Narrow (<1 cm) veins of pale carbonate are widely associated with faults, and bitumen is found in both veins and carbonate mineralized faults. NW-SE trending faults are subsidiary structures and rarely show well-developed kinematic indicators or mineralization.

The most commonly encountered minor structures in the area are small offset faults (Fig. 4e), joints (Fig. 4d) and veins. Generally, fractures and joints are parallel to the major faults and terminate against them or against bedding planes, i.e. they are strata-bound features. Two prominent joint sets are developed trending NNE ranging from 020°

to 050° (mean 025°) and ESE (mean 110°), ranging from 90 to 120°. Dips for both sets range from 50° to vertical.

Isolated small folds (cm to dm scale) occur in the coastal platform. Some are associated with detachments along local fish beds and appear to be early features that are cross-cut by the steeply-dipping NNE-SSW faults (Michie & Bonniface 2009). Others appear to be later brittle-ductile style kink folds with NNE-SSW-trending hinges and ESE dipping axial surfaces (Fig. 4f, g). These folds are locally developed throughout both Caithness and Orkney and are believed to be related to localized deformation during the Late Carboniferous ('Variscan') inversion (e.g. Fletcher & Key 1992, Seranne, 1992). They are cross cut by the NNE-SSW dextral normal faults and their associated carbonate mineralization, including veins.

3.2.3 Minor structures and microstructures exposed in the LLW disposal facility excavations and associated shallow boreholes

The excavations associated with the LLW disposal facilities adjacent to the Dounreay site gave an opportunity in 2012-13 to analyze freshly exposed sections through a number of the NNE-SSW trending fault strands associated with the Gully-Horsetail Fault zone (Fig. 5a,b; Michie & Bonniface 2009). Core samples from four shallow boreholes (BM5.1 BM8.1, GT4 and GT5) drilled prior to the main excavations were also studied (locations shown on Fig 5c). The faults examined here cut through laminated sandstones and siltstones of the Dounreay Shore Formation (Fig. 5b).

In both map and vertical section views, the faults display anastomosing patterns on a number of scales (e.g. Figs. 5c inset, 6a,b) and these are often bounded on either side by larger NNE-SSW trending faults, leading to the development of fracture corridors (cf. Questiaux *et al.* 2010). Some other fault zones show a classical core and damage zone configuration (Fig 6b; Caine *et al.* 1996). The best-defined fracture corridors are typically a few meters wide (Fig. 6a,b) and are likely to be hundreds to thousands of metres long with fracture densities between 3 to 10 fractures/meter. The widespread preferential development of carbonate, base metal sulphide (pyrite, chalcopyrite) and bitumen mineralization along many of the exposed faults indicates that the fault zones have acted as conduits for significant fluid flow in the past.

28 faults and fractures were measured in the excavation exposures. They show a dominant NE to NNE trend with steep (>80°) NW or SE dips (Fig. 6e). A smaller number of NW-SE trending, steeply SW-dipping fractures also occur. Slickenlines on exposed NNE/NE trending faults consistently show dextral oblique extensional kinematics (Fig. 6d). The variable senses of vertical offset seen in the steep excavation walls (e.g. Fig 5b) appear to reflect the consequence of both the dip slip normal and (mainly dextral) strike-slip senses of movement, i.e. the apparently reverse senses of movement are due to displacement in and out of the plane of section.

The exposed faults are widely associated with pale grey-white sparry carbonate (calcite), black bitumen and golden sulphide (pyrite, chalcopyrite) mineralization which is especially well developed along exposed slip surfaces and in small dilational jogs (e.g. Figs 6c,d); the latter preserve rhombohedral zones of mineralized breccia up to 10 cm long and 2 cm wide. Thin sections show that the sulphides present include pyrite (which dominates), fresh chalcopyrite and, in some samples, blue-grey tinged chalcocite, the latter having possibly formed due to the secondary alteration of chalcopyrite (Fig. 7a).

The sulphides are intimately intergrown with calcite or show mutually cross-cutting local overgrowth textures suggesting that these minerals are related to a single phase of contemporaneous mineralization (Figs 7a-c). Vuggy textures are widespread and are displayed by both sulphides and calcite locally (e.g. Figs 7a, c). In many cases, the vugs are filled with bitumen which is also widely seen in late fractures and in areas of locally brecciated carbonate-sulphide fill (e.g. Fig 7d-f). Thus oil fills are consistently the latest seen, but the preservation of oil inclusions within calcite grains (Fig. 7d) suggests that the hydrocarbon charging overlapped with the main phase of mineralization to some extent.

The development of carbonate-sulphide-bitumen mineralization is spectacularly preserved in the shallow borehole cores (Fig 8a-f). Carbonate predominates making up over 80 % by volume of the mineral fills, but minor amounts of sulphide (pyrite, chalcopyrite, chalcocite) and bitumen are also common. Mineralization is seen along lineated shear fractures with the development of oil-stained shear fibres of carbonate intergrown with pyrite showing well-developed steps (Fig 8a). The steep dilational faces of these steps often host small pyrite crystals or oil-filled vuggy cavities (Fig 8b). Widespread centimetre-scale en-echelon dilational veins and hybrid fractures up to 3 cm across are filled with variably brecciated vuggy carbonate, sulphide and bitumen (Fig 8c, d). Individual vuggy cavities in carbonate occur up to 2 cm across and the calcite crystal faces are heavily oil stained and covered in tiny (<1 mm) pyrite crystals (Figs 8e, f). Thin sections show that calcite and the sulphides are closely intergrown and appear to be contemporaneous (Fig. 9a). The majority of oil fills are relatively late and associated with the local reactivation and tensile microbrecciation of existing mineral fills, especially calcite (Figs 9a,b). The microbreccias show little evidence of shear and attrition of clasts and appear to have formed as local explosive hydrofractures. Inspection of fracture-hosted oil fills under higher magnifications and reflected light reveals the presence of numerous tiny (<2 μm) crystals of calcite, pyrite and chalcocite (Figs 9c, d) suggesting that oil charging once again likely overlaps with the main phase of carbonate and sulphide mineralization.

The ubiquity of pyrite-chalcopyrite and especially bitumen in the excavation exposures and shallow borehole cores compared to those exposed on the coast strongly suggests that such mineralization is less frequently seen in coastal outcrops due to the effects of weathering and erosion. Bitumen is prone to being washed away by rain and sea water (biodegraded), whilst pyrite will rapidly degrade to iron oxide. Thus the excavation exposures and cores suggest that the dominant NNE-SSW faults in the region are widely mineralized, and that the products of that mineralization are only occasionally preserved in the otherwise excellently exposed coastal sections.

3.2.4. The White Geos Fault: field relationships and microstructures

The White Geos Fault (WGF) represents one of the better exposed and accessible surface faults in the Dounreay area. It is a subvertical to steeply SE-dipping structure trending NE-SW and is exposed east of Sandside Bay. The fault displaces strata belonging to the Dounreay Shore and Sandside Formations (Fig. 2a). It is easily detectable from aerial photos and its SW and NE intersections with the cliff are marked in plan-view by the development of shallow erosional gully features. It appears to terminate along-strike and to the NE against the Ling Geo Fault (Fig 2a). According to Fletcher & Key (1992), it displays a relatively modest normal (SE-side down) displacement of 1.2 m based on bedding offsets.

The best exposures of the WGF lie half way between its intersection with the cliff and Ling Geo (Fig 10a). Here the deformation is localized in a fault-bounded fracture corridor 2 to 3 meters wide and more than 40 meters long (Fig. 10d). The main fault plane is subvertical to steeply dipping (70°) SE trending NNE (030°). The fault zone comprises in plan-view a series of elongate lenses of relatively undeformed siltstone-sandstone intersliced with lensoid regions of pale carbonate cemented cataclasite-breccia locally up to 15 cm thick, some parts of which carry substantial amounts of sulphide (pyrite, chalcopyrite and chalcocite) which is variably oxidized to red-brown hematite/limonite on exposed surfaces (Fig. 11a-d). Calcite veins up to several cm thick and several metres long are widely developed along many minor NE-SW fractures and more northerly striking carbonate veins that occur in the wall rocks and fault bounded blocks of intact siltstone-sandstone (Fig 10d). The main NE-SW faults contain zones of grey gouge up to several cm thick carrying a fault-parallel shear fabric (NIREX 1994b). These gouges appear to cross cut and rework the other fault rocks and their associated mineralization, and may represent the youngest fault rocks present.

Although fault planes in the cliff and foreshore are heavily weathered and not always well exposed in three dimensions, slickenline lineations are preserved locally. In the sub-horizontal rock platform, small-scale faults show kinematic indicators (grooves, slickenlines) with different orientations (Fig. 11a, b). The majority of NE-SW trending faults show dextral oblique normal displacements. A gentle dm scale open fold occurs south of the main fault (Fig. 10a). The latter is oriented consistent with the overall dextral oblique shear sense of the fault zone (Fig. 10c). Thin tensile veins (< 0.5 cm thick) are observed in the wall rock adjacent to the main faults. Their average trend is NE-SW (subparallel to the strike of the WGF), but curved veins with variable orientations also occur. N-S joints in the fault zone and the adjacent wall rocks are interpreted to be preexisting structures. Some are reactivated as tensile fractures and may show intense localized mineralization (e.g. sulphide at coordinate [40, 4] of Fig. 10d). Locally, later sinistral strike-slip movements are recognized on some of the larger NE-SW trending faults (Fig 11a), and appear to be associated with the development of the youngest clay gouges.

The WGF preserves some of the richest zones of base metal sulphide mineralization seen in the area, preserving well-developed intergrowth textures with each other and with calcite in mineralized breccias of the surrounding country rocks (Figs 12a, b). Once again, oil is a relatively late fill occupying late fractures, breccia zones and vugs in both calcite and sulphide (Figs 11d-f, 12a, c).

4. Rhenium-Osmium Geochronology

4.1 Samples

The field, hand sample and microstructural studies have shown that in all locations studied, the sulphide mineralization was synchronous with both carbonate mineralization and faulting. The pyrites found within these samples are ideal candidates for dating as constraining the date of mineralization in this instance also constrains the timing of fault activity. A suite of 8 pyrite samples were collected from unweathered materials preserved in the excavations and borehole cores. Six of these samples possessed sub 100 ppt (parts per trillion) rhenium and were not considered capable of yielding precise Re-Os dates.

The remaining two pyrite samples (RO512-7_py D2 and RO531-2_DR4) possessed parts per billion (ppb) rhenium levels. These two pyrite samples analysed come from two larger NNE-SSW fault zones seen cutting the southwestern wall of the excavations (for precise locations see Fig 5d). In both cases, the pyrite is intergrown with calcite in well-defined dilational jogs (one of which is shown in Fig 6c).

4.2. Rhenium-Osmium analytical protocols

Rhenium-osmium isotopic analyses were conducted at the Laboratory for Sulphide and Source Rock Geochronology, and Geochemistry at Durham University (part of the Durham Geochemistry Centre). The pyrite samples were isolated from the vein host material by crushing, without metal contact, to a < 5 mm grain size. After this stage approximately 1 g of pyrite was separated from the crushed vein by hand picking under a microscope to obtain a clean mineral separate. The analytical protocols followed those of Selby *et al.* (2009). In brief, ~ 0.4 g of accurately weighed pyrite was loaded into a carius tube with a known amount of a mixed ^{185}Re and $^{188}Os+^{190}Os$ tracer (spike; Markey *et al.*, 2007) solution together with 11 ml of inverse *aqua regia* (3 ml 11N HCl and 8 ml 15 N HNO_3). The carius tubes were then sealed and placed in an oven at 220°C for 48 hrs. Osmium from the acid medium was extracted using $CHCl_3$ solvent extraction and further purified using micro-distillation. Rhenium from the remaining acid medium was isolated via NaOH-Acetone solvent extraction and anion exchange column chromatography (Cumming *et al.*, 2013). The purified Re and Os fractions were then loaded onto Ni and Pt filaments, respectively, and analysed for their isotope compositions using negative-ion mass spectrometry on a Thermo Scientific TRITON mass spectrometer. Rhenium isotopes were measured using Faraday Collectors, with osmium isotope compositions determined using a Secondary Electron Multiplier. Total procedural blanks for Re and Os are 3.5 ± 2 pg and 0.2 ± 0.15 pg, respectively, with an average $^{187}Os/^{188}Os$ of 0.25 ± 0.02 (n = 2, 1 SD). In addition to these, Re and Os standard solution measurements were performed during the two mass spectrometry runs (Re std = 0.5987 ± 0.0011; DROsS (Osmium Standard) = 0.1602 ± 0.0002. These values are within agreement of those reported by Finlay *et al.* (2011) and references therein.

4.3. Results

The Re and Os uncertainties presented in Table I were determined by the full propagation of uncertainties from the mass spectrometer measurements, blank abundances and isotopic compositions, spike calibrations, and the results from analyses of Re and Os standards. The Re standard data together with the accepted $^{185}Re/^{187}Re$ ratio (0.59738; Gramlich *et al.*, 1973) were used to correct for mass fractionation.

The total Re and Os abundances of the pyrite samples range from 9.1 to 35.7 ppb and 26.5 to 100.8 ppt (Table I), respectively. The majority of the Os within the pyrite samples is radiogenic $^{187}Os^{r}$ (99 and 98 % in samples RO512-7_py D2 and RO531-2_DR4, respectively) with only very minor amounts of unradiogenic common osmium present (≤ 2 %). Consequently the Re-Os systematics of the pyrite are akin to those of molybdenite (Stein *et al.*, 2001), and the predominance of $^{187}Os^{r}$ in the pyrite samples defines them as Low Level Highly Radiogenic (LLHR; Stein *et al.*, 2000; Morelli *et al.*, 2005). Therefore using the standard equation $t = \ln(^{187}Os^{r}/^{187}Re = 1) / \lambda$ model Re-Os dates for each sample can be calculated independently, identical to those determined for molybdenite. The model Re-Os dates for RO512-7_pyD2 and RO531-2_DR4 are identical within uncertainty (268.4 ± 4.8 [4.9] Ma and 266.4 ± 5.1 [5.2] Ma; bracketed numbers include both the analytical and decay constant uncertainties, respectively; Table 1), and suggest that sulphide mineralization occurred broadly contemporaneously. A weighted average of the two Re-Os model ages is 267.5 ± 3.4 [3.5] Ma (MSWD = 0.29; Fig. 13). We use this age to define the timing of sulphide mineralization at the fresh excavation exposures and, by inference, that of the other vein hosted minerals and associated faulting at 267.5 ± 3.4 [3.5] Ma.

5. Discussion

5.1. The age of the main phase of faulting in the Dounreay district and Caithness

Our field, microstructural and geochronological findings suggest that the dominant set of regional faults cutting the Devonian Orcadian Basin sedimentary rocks in the Dounreay district formed during the Lower Permian (ca. 267 Ma). This event was associated with widespread carbonate-base metal sulphide mineralization, which was shortly followed by the influx of small, but regionally persistent amounts of fracture-hosted hydrocarbons. The Middle Devonian shale and fish bed sequences of the Caithness Orcadian Basin are known to be good potential hydrocarbon sources (e.g. see Parnell 1985; Marshall *et al* 1985) and so it seems likely that oil hosted in the fractures is of local derivation. The proposed timing of oil generation is consistent with apatite fission track analyses (Thomson *et al.* 1999), which suggest that maximum palaeotemperatures were attained across Northern Scotland between the early Carboniferous and mid-Triassic. Interestingly, the ca. 267 Ma Re-Os pyrite age at Dounreay overlaps with K-Ar ages of

268-249 Ma (Baxter & Mitchell 1984) from three alkaline lamprophyre dykes in the Thurso region immediately to the east. More generally, this timing also coincides with the latest peak of mantle-sourced regional Permian (ca 269-261 Ma) igneous activity throughout NW Europe and the North Sea (see Glennie *et al.* 2003; Upton *et al.* 2004). It is therefore conceivable that sulphide mineralization and possibly local oil generation are related to regional igneous and/or hydrothermal activity.

5.2. Stress inversion and paleostress analysis

Modern stress inversion techniques calculate the stress tensor associated with a set of coeval kinematic indicators (e.g. slickenlines) measured directly from sets of related fault surfaces. All stress inversion techniques assume a statistical parallelism between the observed slip vector (measured on fault surfaces) and the model shear traction (shear component of stress tensor, resolved on a particular fault plane via Cauchy's double dot product) (Wallace 1951; Bott 1959). This suggests that for faults to be suitable for this kind of analysis, displacements must be small; i.e. low infinitesimal strain and little or no rotational strain.

Several graphical and numerical approaches have been proposed (e.g. Angelier & Mechler, 1977; Etchecopar *et al.*, 1981; Angelier, 1991; Michael, 1984; Reches, 1987; Yamaji, 2000; Delvaux & Sperner, 2003). Generally the analysis produces a reduced stress tensor with just four parameters (Etchecopar *et al.,* 1981): the orientation of the three principal axes (σ_1, σ_2 and σ_3) and the shape factor $\delta = (\sigma_2 - \sigma_3) / (\sigma_1 - \sigma_3)$. This tensor represents, in a dimensional form, the deviatoric component of the total stress tensor; the isotropic component does not influence shear stress on fault surfaces. Ideally, the most robust numerical solution requires at least four statistically independent structure sets to be measured (see Angelier, 1991). While the structures analysed herein are predominantly NNE-SSW striking there is sufficient scatter to meet this criterion.

Fault-slip slickenline data were collected *in-situ* and conventional stress inversion techniques (Angelier, 1979, 1984; Michael, 1984) were carried out using MyFault® software to calculate the minimized shear stress variation. This method assumes that all slip events are independent but occur as a result of a single stress regime. The small (<5 metre) displacements observed on most of the mineralized structures allow us to infer that the regional strain intensities were low and the degree of rotational strain negligible. 132 faults were measured during this study (Fig.14a), of which 25 were striated and mineralized (Fig. 14b). The results of this analysis show that at the time of mineralization the studied fault zones were undergoing dextral transtension (δ = 0.22) with principal extension (σ_3) towards 315° (Fig 14b). The associated Mohr Circle plot (Fig 14b) shows that the structures analysed for this study were particularly well-orientated for both shear and tensional failure.

5.3. Regional implications

Regional mapping in the Dounreay district and adjacent parts of Caithness (e.g. Fletcher & Key 1992; NIREX 1994a-c, BGS 1985, 2005) suggest that major changes in thickness and/or Devonian stratigraphy occur across a number of the larger N-S to NNE-SSW faults including the Bridge of Forss and Dog Track Faults (Fig. 2a, b). Given their influence on the Orcadian Basin fills, it seems likely that these faults formed in the Devonian and were reactivated during later Permian and possibly younger movements.

However, the great majority of faults and fractures in the Dounreay district appear to have formed in association with base metal sulphide, carbonate and possibly overlapping late oil mineralization ca 267 Ma. Our new findings add to an increasing body of evidence suggesting that the onshore normal faulting in Sutherland and Caithness is dominated by structures related, and peripheral, to the offshore Permo-Triassic West Orkney Basin (e.g. Roberts & Holdsworth 1999; Blumstein *et al.* 2005; Wilson *et al.* 2010; Elmore *et al.* 2010). Wilson *et al.* (2010) proposed the existence of a broad ESE-WNW-trending zone of transtensional faulting – the North Coast Transfer Zone (Fig. 15a,b). It comprises a diffuse system of synthetic ESE-WNW sinistral and antithetic N-S to NE-SW dextral extensional faults. The predominantly dextral-extensional N-S to NE-SW faults of the Dounreay district and adjacent parts of Caithness are plausibly an eastward continuation of this zone, the dominance of dextral antithetic structures possibly reflecting preferential reactivation of fault trends first established in the Devonian during the initial development of the Orcadian Basin. It seems likely that the intensity of deformation associated with the NCTZ may progressively weaken eastwards as it acts principally to transfer Permian to Triassic extension in the West Orkney Basin westwards and into the North Minch Basin (Fig. 15b).

Conclusions

The Middle Devonian rocks of the Orcadian Basin of northernmost Caithness (in the Dounreay district) are cut by a series of N to NE striking faults. These brittle structures are characteristically associated with widespread carbonate-base metal sulphide (pyrite, chalcopyrite, chalcocite)-hydrocarbon mineralization hosted in tensile veins, dilational jogs and along shear surfaces.

Field and microstructural observations show that the carbonate and sulphide mineralization is coeval and occurred synchronously with the main phase of dextral transtensional fault movements on these structures. Hydrocarbons originating from local Devonian source rocks consistently post-date local carbonate and pyrite fills, but are hosted in the same fracture systems and likely overlapped in time with the main phase of mineralization and faulting. Stress inversion analyses carried out on slickenline-bearing mineralized faults in the region suggest that they are associated with a regional phase of NW-SE extension.

Re-Os geochronology carried out on two samples of fault-hosted pyrite yield a weighted average model age of 267.5 ± 3.4 [3.5] Ma. This suggests that the main phase of extensional-transtensional faulting cutting the Devonian rocks of the Dounreay district – and by inference a substantial part of Caithness - is mid-Permian. This timing, coupled with the NW-SE regional extension direction, agrees with onshore studies in Sutherland suggesting that the dominant set of faults seen along the north coast of Scotland formed part of a regional structure located on the southern periphery of the offshore West Orkney Basin: the North Coast Transfer Zone (Fig. 15 a, b). Thus, it appears that the brittle faulting seen in Precambrian to Devonian rocks exposed along the entire length of the north coast of Scotland is related principally to the tectonic development of latest Palaeozoic to Mesozoic basins presently located offshore. The total amount of onshore extension at this time is difficult to estimate with any degree of confidence, but it is likely to be significantly less than that seen in the West Orkney Basin offshore since most of this deformation is transferred west into the North Minch Basin (Fig. 15b).

Finally, there is no compelling evidence for Jurassic or younger faulting in the north coastal region of Caithness, despite the relative proximity of the Inner Moray Firth Basin where extension of these ages is widely documented (e.g. see Le Breton *et al.* 2013 and references therein). This suggests that the Helmsdale Fault and northern continuation of the Great Glen Fault offshore (Fig. 1a) may form an effective northwestern limit of Jurassic extension and younger faulting events, a proposal that remains to be tested through further work.

Acknowledgements

This research is based on the PhD work of AD funded by the Clair Joint Venture Group (BP, Shell, ConocoPhillips, Chevron). Simon Richardson and Andy Conway are thanked for their long-standing support of the Durham research Group. Ian Chaplin is thanked for his outstanding thin section preparation and Leon Bowen for his help with SEM work. We are very much indebted to Alan Roberts, Graham Leslie and Woody Wilson for their critical comments and inputs that have led to significant improvements in the paper.

References

Angelier J., 1979. Determination of the mean principal directions of stresses for a given fault population. *Tectonophysics*, 56(3):T17–T26.

Angelier J., 1984. Tectonic analysis of fault slip data sets. *Journal of Geophysical Research: Solid Earth (1978–2012)*, 89(B7):5835–5848.

Angelier J., 1991. Inversion directe et recherche 4-d: comparaison physique et mathématique de deux modes de détermination des tenseurs des paléocontraintes en tectonique de failles. *Comptes rendus de l'Académie des sciences. Série 2, Mécanique, Physique, Chimie, Sciences de l'univers, Sciences de la Terre*, 312(10):1213–1218.

Angelier J. & Mechler P., 1977. Sur une méthode graphique de recherche des contraintes principales également utilisable en tectonique et en séismologie: la méthode des diédres droits. *Bulletin de la Société Géologique de France*, XIX(6):1309–1318.

Baxter, A.N. and Mitchell, J.G. 1984. Camptonite-monchiquite dyke swarms of Northern Scotland; age, relationships and their implications. *Scottish Journal of Geology*, 20, 297-308.

BGS. 1985. *Reay, Scotland Sheet 115E. Solid Geology. 1:50,000.* British Geological Survey, Keyworth, Nottingham.

BGS. 2005. *Dounreay Scotland, parts of sheet ND06 and ND07 Bedrock.* 1:25000 Geology Series, British Geological Survey, Keyworth, Nottingham.

Blumstein R.D., Elmore R.D., Engel M.H., Parnell J., and Baron M., 2005. Multiple fluid migration events along the Moine Thrust Zone, Scotland. *Journal of the Geological Society*, 162(6):1031–1045.

Bott M.H.P., 1959. The mechanics of oblique slip faulting. *Geological Magazine*, 96(02):109–117.

Brewer J.A. & Smythe D.K., 1984. MOIST and the continuity of crustal reflector geometry along the Caledonian-Appalachian orogen. *Journal of the Geological Society*, 141(1):105–120.

Caine, J.S., Evans, J.P., Forster, C.B., 1996. Fault zone architecture and permeability structure. *Geology* 24, 1025–1028.

Coward, M.P. & Enfield, M.A. 1987. The structure of the West Orkney and adjacent basins. In: Brooks, J.V. & Glennie, K.W. (eds) *Petroleum Geology of North West Europe*. Proc. of the 3rd Conference on Petroleum Geology of North West Europe. Graham & Trotman, 687 - 696.

Coward M.P., Enfield M.A., and Fischer M.W., 1989. Devonian basins of Northern Scotland: extension and inversion related to Late Caledonian-Variscan tectonics. *Geological Society, London, Special Publications,* 44(1):275–308.

Cumming, V.M., Poulton, S.W., Rooney, AD., Selby, D., 2013. Anoxia in the terrestrial environment during the Late Mesoproterozoic. *Geology,* doi:10.1130/G34299.1.

Delvaux D. & Sperner B., 2003. New aspects of tectonic stress inversion with reference to the TENSOR program. *Geological Society, London, Special Publications*, 212(1):75–100.

Dempsey E.D., Holdsworth R.E., Imber J., Bistacchi A., and Di Toro G., 2014. A geological explanation for intraplate earthquake clustering complexity: The zeolite-bearing fault/fracture networks in the Adamello Massif (Southern Italian Alps). *Journal of Structural Geology*, 66:58–74.

Dewey J.F. & Strachan R.A., 2003. Changing Silurian-Devonian relative plate motion in the Caledonides: sinistral transpression to sinistral transtension. *Journal of the Geological Society*, 160(2):219–229.

Duncan W.I. & Buxton N.W.K., 1995. New evidence for evaporitic Middle Devonian Lacustrine sediments with hydrocarbon source potential on the East Shetland Platform, North Sea. *Journal of the Geological Society*, 152(2):251–258.

Elmore R.D., Burr R., Engel M., and Parnell J., 2010. Paleomagnetic dating of fracturing using breccia veins in Durness group carbonates, NW Scotland. *Journal of Structural Geology*, 32(12): 1933 – 1942.

Enfield M.A. & Coward M.P., 1987. The structure of the West Orkney Basin, northern

Scotland. *Journal of the Geological Society*, 144, 871–884.

Etchecopar A., Vasseur G., and Daignieres M., 1981. An inverse problem in microtectonics for the determination of stress tensors from fault striation analysis. *Journal of Structural Geology*, 3, 51–65.

Evans, D., Graham, C., Armour, A. Grahman, C. and Bathurst, P. 2003. *The Millennium Atlas: Petroleum Geology of the Central and Northern North Sea*. Geological Society, London, 390 pp.

Finlay A. J., Selby D., and Osborne M. J., 2011. Re-os geochronology and fingerprinting of United Kingdom Atlantic margin oil: Temporal implications for regional petroleum systems. *Geology,* 39(5):475–478.

Finlay A.J., Selby D., and Osborne M.J, 2012. Petroleum source rock identification of United Kingdom Atlantic Margin oil fields and the Western Canadian Oil Sands using Platinum, Palladium, Osmium Andrhenium: Implications for global petroleum systems. *Earth and Planetary Science Letters*, 313-314 (0):95 – 104. ISSN 0012-821X.

Fletcher T.P. & Key R.M., 1992. Solid geology of the Dounreay district. *British Geological Survey Technical Report, WA/91/35,* 143pp.

Friend C.R.L., Jones K.A., and Burns I.M., 2000. New high-pressure granulite event in the Moine Supergroup, northern Scotland: Implications for Taconic (early Caledonian) crustal evolution. *Geology*, 28(6):543–546.

Gramlich J.W., Murphy T.J., Garner E.L., and Shields W.R., 1973. Absolute isotopic abundance ratio and atomic weight of a reference sample of rhenium. *J. Res. Natl. Bur. Stand*. A, 77:691–698.

Glennie, K.W., Higham, J. and Stemmerik, L. 2003. Permian. *In:* Evans, D., Graham, C., Armour, A. and Bathurst, P. (eds) *Millenium Atlas: Petroleum Geology of the northern North Sea*, 91-103.

Holdsworth, R.E., Dempsey, E., Selby, D., Darling, J.R., Feely, M., Costanzo, A., Strachan, R.A., Waters, P., Finlay, A.J. and Porter, S.J. 2015. Silurian–Devonian magmatism, mineralization, regional exhumation and brittle strike-slip deformation along the Loch Shin Line, NW Scotland. *Journal of the Geological Society,* 172, doi:10.1144/jgs2015-058

Imber J., Holdsworth R. E., Butler C. A., and Strachan R. A., 2001. A reappraisal of the Sibson-Scholz fault zone model: The nature of the frictional to viscous (brittle-ductile) transition along a long-lived, crustal-scale fault, Outer Hebrides, Scotland. *Tectonics*, 20(5):601–624.

Johnstone G.S. & Mykura W., 1989.*The Northern Highlands of Scotland*. British Regional Geology (4th Edition), British Geological Survey, HMSO London.

Kocks H., Strachan R.A., and Evans J.A., 2006. Heterogeneous reworking of Grampian metamorphic complexes during Scandian thrusting in the Scottish Caledonides: insights from the structural setting and U-Pb geochronology of the Strath Halladale Granite. *Journal of the Geological Society,* 163, 525–538.

Le Breton E., Cobbold, P.R., Zanella, A.,2013. Cenozoic reactivation of the Great Glen Fault, Scotland: Additional Evidence and Possible Causes. *Journal of the Geological Society, London,* 170, 403-415. doi: 10.1144/jgs2012-067.

Markey, R.J., Stein, H.J., Hannah, J.L., Zimmerman, A., Selby, D., and Creaser, R.A., 2007, Standardizing Re-Os geochronology: A new molybdenite reference material (Henderson, USA) and the stoichiometry of Os salts: Chemical Geology, v. 244, p. 74-87.

Marshall J.E.A. & Hewett A.J., 2003. Devonian. *In:* Evans, D., Graham, C., Armour, A. and Bathurst, P. (eds) *Millenium Atlas: Petroleum Geology of the northern North Sea*, 64-81.

Marshall, J.E.A., Brown, J.F. and Hindmarsh, S. 1985. Hydrocarbon source rock potential of the Devonian rocks of the Orcadian Basin. Scottish Journal of Geology, 21, 301-320.

McClay K., Norton M.G., Coney P. and Davis G.H. 1986. Collapse of the Caledonian orogen and the Old Red Sandstone, Nature, London, 323, 147-149.

Michael A.J., 1984. Determination of stress from slip data: faults and folds. *Journal of Geophysical Research: Solid Earth (1978–2012),* 89(B13):11517–11526.

Michie, U. & Bonniface, J. 2010. *Geology and Structure: Update from 2009 Site Characterisation.* New Low Level Waste Facilities Report NLLWF/3/REP/QNT/0120/IS/01, Dounreay Scotland, pp60.

Morelli, R.M., Creaser, R.A., Selby, D., Kelley, K.D., Leach, D.L., and King, A.R., 2004, Re-Os sulfide geochronology of the Red Dog sediment hosted Zn-Pb-Ag deposit, Brooks Range, Alaska: Economic Geology, v. 99, p. 1569-1576.

Morelli R.M., Creaser R.A., Selby D., Kontak D.J., and Horne R.J., 2005. Rhenium-osmium geochronology of arsenopyrite in Meguma Group gold deposits, Meguma Terrane, Nova Scotia, Canada: evidence for multiple gold-mineralizing events. *Economic Geology*, 100(6):1229–1242.

NIREX, 1994a. The geology of the region around Dounreay: Report of the Regional Geology Joint Interpretation Team. Lead Authors: Holliday D.W. and Holmes D.C.*UK Nirex Limited Report. 657.*

NIREX, 1994b. Dounreay Geological Investigations: District Geology. *Technical report, UK Nirex Limited Report. 658.*

NIREX, 1994c. Dounreay Geological Investigations: Geological Structure. *Technical report, UK Nirex Limited Report. 659.*

Norton M.J., McClay K.R., and Nick A.W., 1987. Tectonic evolution of Devonian basins in northern Scotland and southern Norway. *Norsk Geologisk Tidsskrift,* 67, 323-338.

Parnell, J. 1985. Hydrocarbon source rocks, reservoir rocks and migration in the Orcadian Basin, *Scotland. Scottish Journal of Geology*, 21, 321-336.

Passchier C.W. and Trouw R.A.J., 2005. Microtectonics, 366 pp.

Questiaux J., Couples G.D., and Ruby N., 2010. Fractured reservoirs with fracture corridors. *Geophysical Prospecting*, **58**, 279–295.

Reches Z., 1987. Determination of the tectonic stress tensor from slip along faults that obey the Coulomb yield condition. *Tectonics,* 6, 849–861.

Roberts, A.M. & Holdsworth R.E., 1999. Linking onshore and offshore structures: Mesozoic extension in the Scottish Highlands. *Journal of the Geological Society*, 156, 1061–1064.

Rogers D.A., Marshall J.E.A., and Astin T.R., 1989. Short paper: Devonian and later movements on the Great Glen fault system, Scotland. *Journal of the Geological Society,* 146, 369–372.

Selby D., Kelley K. D., Hitzman M. W., and Zieg J., 2009. Re-Os sulfide (bornite, chalcopyrite, and pyrite) systematics of the carbonate-hosted copper deposits at Ruby Creek, Southern Brooks Range, Alaska. *Economic Geology*, 104, 437–444.

Seranne M., 1992. Devonian extensional tectonics versus Carboniferous inversion in the northern Orcadian basin. *Journal of the Geological Society*, 149, 27–37.

Sibson R.H., 1977. Fault rocks and fault mechanisms. *Journal of the Geological Society,* 133, 191–213.

Stein, H. J., Markey, R. J., Morgan, J. W., Hannah, J. L. & Schersten, A. The remarkable Re-Os chronometer in molybdenite: how and why it works. *Terra Nova* **13**, 479-486 (2001).

Stein H.J., Morgan J.W., and Scherstén A., 2000. Re-Os dating of low-level highly radiogenic (llhr) sulfides: The Harnäs gold deposit, Southwest Sweden, records continental-scale tectonic events. *Economic Geology*, 95, 1657–1671.

Stoker M.S., Hitchen K., and Graham C.C. 1993. *The Geology of the Hebrides and West Shetland Shelves, and Adjacent Deep Water Areas.* British Geological Survey Offshore Regional Report, HMSO, London.

Thomson, K., Underhill, J.R., Green, P.F., Bray, R.J. and Gibson, H.J. 1999. Evidence form fission track analysis for the post-Devonian burial and exhumation history of the Northern Highlands, Scotland. *Marine and Petroleum Geology,* 16, 27-39.

Upton, B.D.J, Stephenson, D., Smedley, P.M., Wallis, S.M., and Fitton. G.J. 2004. Carboniferous and Permian magmatism in Scotland. *In:* Wilson,M., Neumann, E-R., Davies, G.R., Timmerman, M.J., Heeremans, M., and Larsen, B.T. (eds.) *Permo-Carboniferous Magmatism and Rifting in Europe*, Geological Society of London, Special Publications 223, 219–242.

van der Pluijm B.A., Hall C.M., Vrolijk P.J., Pevear D.R., and Covey M.C., 2001. The dating of shallow faults in the Earth's crust. *Nature*, 412, 172–175.

Vernon R., Holdsworth R.E., Selby D., Dempsey E., Finlay A.J., and Fallick A.E., 2014. Structural characteristics and Re–Os dating of quartz-pyrite veins in the Lewisian Gneiss Complex, NW Scotland: Evidence of an early Paleoproterozoic hydrothermal regime during terrane amalgamation. *Precambrian Research*, 246, :256–267.

Wallace R.E., 1951. Geometry of shearing stress and relation to faulting. *The Journal of Geology*, 118–130.

Watts L.M., Holdsworth R.E., Sleight J.A., Strachan R.A., and Smith S.A.F., 2007. The movement history and fault rock evolution of a reactivated crustal-scale strike-slip fault: the Walls Boundary Fault Zone, Shetland. *Journal of the Geological Society*, 164(5):1037–1058, 2007.

Wilson R.W., Holdsworth R.E., Wild L.E., McCaffrey K.J.W., England, R.W, Imber, J. and Strachan, R.A. 2010. Basement influenced rifting and basin development: a reappraisal of post-Caledonian faulting patterns from the North Coast Transfer Zone, Scotland. *Geological Society, London, Special Publications* 335, 795–826.

Woodcock, N.H. and Strachan, R.A. (eds) 2012. Geological History of Britain and Ireland (Second Edition). John Wiley & Sons.

Yamaji A., 2000. The multiple inverse method: a new technique to separate stresses from heterogeneous fault-slip data. *Journal of Structural Geology*, 22, 441–452.

FIGURES

Figure 1: (a) Regional geological map of Northern Scotland and associated offshore regions adapted from Evans *et al.* (2003) showing the main basins, regional fault systems, offshore seabed outcrops and onshore Devonian sedimentary outcrops. NHT = Northern

Highland Terrane; CHT = Central Highland Terrane; O = Orkney; S = Shetland; DH = Dunnet Head. (b) Simplified reconstruction of the palaeocontinental fragments around Britain, East Greenland and Norway prior to continental break up and opening of the Atlantic (Woodcock & Strachan, 2012 modified). Yellow star shows the area of study.

Figure 2: (a) Onshore geological map of the Dounreay coastal region (after BGS 2005) combined with nearshore bathymetric image coloured for depth. (b) Cross-section intersecting the Nirex BH1 and BH2 boreholes (modified after BGS 2005) – line of section shown in a). Boxes show location of maps shown in Figs 5a and 7a.

Figure 3: Rose diagrams of azimuth distributions (left) and azimuth/length distributions (right) of: (a) interpreted lineaments from Getmapping aerial images; (b) interpreted lineaments from bathymetric data; (c) faults in existing geological maps; and (d) all lineaments and fault data. For each diagram, rose diagram statistics and relative maximum (red arrow) are shown. For lineament maps, see Appendix A.

Figure 4: Structures developed in the coastal exposures of the Dounreay area. (a) Typical example of heavily eroded fault zone coastal gully known as a "geo" (NC 99377 68089). (b) ESE-dipping normal fault plane with breccia patch developed in a relay zone with well-developed near dip-slip slickenlines (arrowed; NC 99375 68080). (c) 1cm thick carbonate mineralization along an exposed WNW-dipping fault surface with dextral oblique slickenfibres parallel to pen (NC 99314 68011). (d) Well-developed fractures and joints developed within a bedding plane with rose diagram. (e) Small scale faults with drag features associated with small relay zones (NC 99330 68052). (f) Small NNE-plunging brittle-ductile fold pair (NC 99300 68000). (g) Stereonets of structural data

collected on the shore section between the Dog Track and Geodh nam Fitheach faults. (1) Poles to bedding and contoured density plot. (2) Poles to faults and fractures and relative density plot. (3) Poles to fold hinges and axial planes and density plot of fold hinges.

Figure 5: (a, b) Oblique aerial photographs of the Dounreay coast and recent excavations near the nuclear research establishment. (c) Geological map of the inland Dounreay area and in inset map, detail of the excavations showing main faults and shallow borehole locations. Note oblique orientation of north arrow. (d) SE-NW face of the SW wall of the southernmost excavation (location in shown in c) showing major faults and the location of the samples collected for Re-Os dating.

Figure 6: Outcrop photos from the Dounreay excavations showing: (a) Well developed NNE-SSW fracture corridor. Most fractures are confined between two bounding faults (thicker red lines). (b) Fault core and damage zones. (c) 3cm thick dilational jog with carbonate and sulphide mineralization and solid bitumen. Vuggy voids are also preserved in the jog. (d) Oblique kinematics on a NNE-SSW trending fault (footwall face) showing carbonate fibres and bitumen staining (compass for scale). (e) Equal area stereonet plots of structural data collected in the excavations. Poles to faults and fractures and relative density plot.

Figure 7: Representative thin-section photomicrographs of a fault samples collected in the excavations showing: (a) typical mineralized breccia with rounded to angular clasts of wall rock with halos of golden pyrite (Py), blue-gold chalcocite (Ch) likely after chalcopyrite and calcite (Ca). (b) Detailed view of country rock clast cut by vein of early calcite and pyrite cross cut by Pyrite halo round clast and later calcite vuggy fill. (c)

Clasts of country rock with pyrite halos and later calcite vuggy infill with oil inclusions in calcite towards the centre of the vug. (d-f) Representative microphotographs showing typical occurrence of bitumen in pre-existing calcite-sulphide-filled fractures and vugs. Images in (b-f) are in PPL.

Figure 8: Borehole cores samples showing well preserved mineralization and associated faulting-fracturing. (a, b) Slickenfibre lineations (red dashed lines) on shear fractures, with calcite, pyrite and bitumen in dilational jogs/fiber steps. (c, d) En echelon dilational veins and hybrid fractures filled with variably brecciated vuggy carbonate, sulphide and bitumen. (e) Fracture and vuggy dilational jogs with fractured and heavily oil stained calcite crystals. (f) Detailed internal view of 2 cm wide vuggy cavity with large calcite crystal faces coated with oil and numerous tiny pyrite crystals.

Figure 9: (a) Representative thin-section of explosive fault breccia in dilational jog. The clasts in the breccia are formed almost totally by calcite mineralization with interstitial spaces filled with bitumen. OSCB = Oil-stained calcite breccia; Ca = calcite; WR = wall rocks. (b) Detailed PPL view of oil-filled microbreccia in rhombochasm. (c) High power transmitted light PPL view of oil-filled fractures in calcite grain. Location of image in (d) is also shown. (d) High power reflected light close-up of oil (grey)-filled microcavity with numerous tiny crystals of pyrite (gold), chalcocite (blue) and calcite (white). All images are from borehole BM8.1 at 16.6 m depth.

Figure 10: (a) Getmapping plc aerial image of the White Geo fault with local geology (see Fig 2). (b) NW-SE cross-section view of the fault zone in coastal cliff. (c) Oblique view of the fault zone showing details of the structures in part of the coastal platform. (d)

Detailed geological map of the White Geo Fault Zone including the location of Figs b and c. Also includes locality stereoplots and fault data and fault kinematics. Note that N in the stereonets is rotated into parallelism with the N grid of the map for ease of viewing.

Figure 11: Field photographs from the White Geo Fault Zone. (a) Sinistral strike-slip grooves on exposed NE-SW trending faults (coin for scale). (b) Dextral-oblique kinematics on a NE-SW fault plane and (c) sinistral-oblique ENE-WSW fault with associated carbonate mineralization and hematite staining (compass for scale) (both from NC 9699 6644). (d) Plan view of a fault breccia with intense carbonate-sulphide mineralization. (e) Freshly broken open surface of fault rocks showing zones of early sulphide overgrown by calcite lining a bitumen-filled vuggy cavity. (f) Sulphide-rich fault zone with characteristic hematite staining due to oxidation and weathering. (g) Equal area stereonet plots of structural data collected in the White Geo Fault zone: (1) Poles to bedding (grey dots) and relative density plot. (2) Poles to veins (blue triangles) and relative density plot. (3) Poles to fault and fractures planes (red dots) and relative density plot.

Figure 12: (a) Small cut sample of mineralized breccia from the White Geo Fault Zone consisting of pyrite (Py), chalcopyrite (Cp), pale calcite (Ca) and oil stained calcite breccia (OSCB). (b) Detailed image of well-developed sulphide intergrowth textures with each other and calcite in mineralized breccias. (c) SEM microphotograph showing oil infilling microbreccia of intergrown pyrite and calcite.

Figure 13: Re-Os isochron and model age plots for pyrite samples PyD2 and DR4. See Figure 5d for location of samples.

Figure 14: (a) Equal area stereoplots of poles to all fault and fractures measured in the Dounreay district (red dots) and relative density plot. (b) (left) Combined density plot of mineralized fault planes, with slip lineations (red dots) and stress inversion indicating a regional NW-SE extension. (right) Mohr plot showing an intermediate stress value (0.72) typical of transtensional regime and that most of the analysed shear plans are well oriented for slip.

Figure 15: a) Simplified geological map showing the proposed location of the Permian to Triassic North Coast Transfer Zone (NCTZ) that forms along the southern periphery of the offshore West Orkney Basin (after Wilson et al. 2010). b) Schematic 3D figure showing how the NCTZ acts to transfer extension in the West Orkney Basin (WOB) westwards into the North Minch Basin (NMB). Note that the intensity of deformation along the NCTZ is shown as decreasing eastwards. Drawn looking towards the northwest. GGFZ = Great Glen Fault Zone; MFZ = Minch Fault Zone. Dashed box shows location of map in a).

Table 1: Re-Os data obtained from freshly exposed pyrite samples retrieved from fault infills exposed in LLW facility excavations**.**

Table 1. Re-Os data for pyrite from Dounreay

Sample	Wt (g)	Re (ppb)	±	^{187}Re (ppb)	±	^{187}Os^{r} (ppt)	±	^{187}OsC* (ppt)	±	OsC^ (ppt)	±	Age§ (Ma)	±	± decay constant
RO512-7_pyD2	0.40	9.11	0.12	5.73	0.08	25.66	0.29	0.09	0.07	0.59	0.20	268.4	4.8	4.9
RO531-2_DR4	0.40	35.65	0.53	22.41	0.33	99.70	1.23	0.09	0.05	0.99	0.20	266.4	5.1	5.2

*abundance of radiogenic ^{187}Os (^{187}Os^{r}) and non radiogenic ^{187}Os (^{187}OsC)
^abundance of Total non-radiogenic Os
§Uncertainty in the age are presented to include all sources of analytical uncertainty with and without the uncertainty in the decay constant (λ).

Figure 1

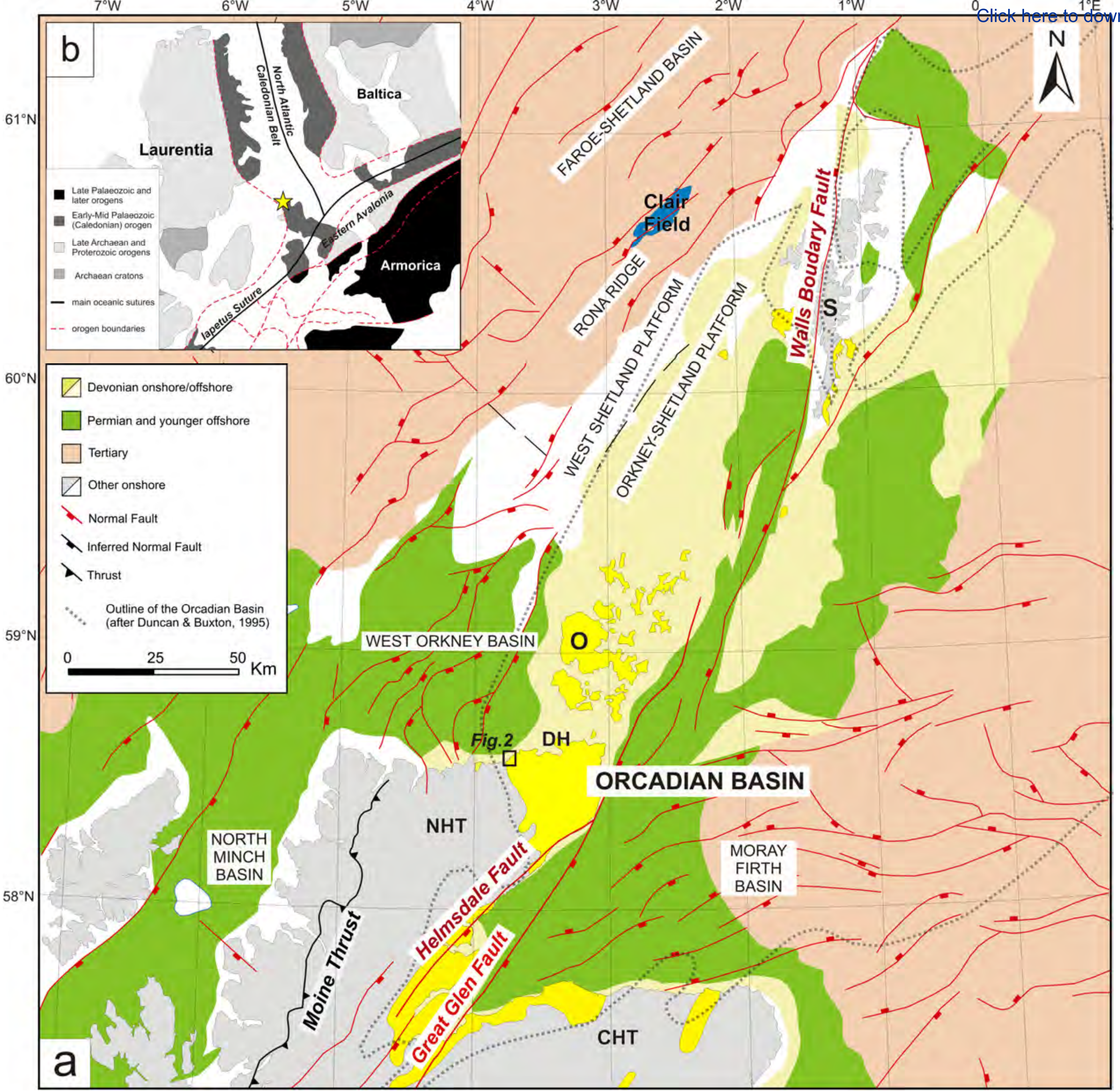

7°W
6°W
5°W
4°W
3°W
2°W
1°W
0
1°E
61°N
60°N
59°N
58°N
N
b
Laurentia
Baltica
Armorica
North Atlantic Caledonian Belt
Eastern Avalonia
Iapetus Suture
Late Palaeozoic and later orogens
Early-Mid Palaeozoic (Caledonian) orogen
Late Archaean and Proterozoic orogens
Archaean cratons
main oceanic sutures
orogen boundaries
Devonian onshore/offshore
Permian and younger offshore
Tertiary
Other onshore
Normal Fault
Inferred Normal Fault
Thrust
Outline of the Orcadian Basin (after Duncan & Buxton, 1995)
0
25
50
Km
FAROE-SHETLAND BASIN
Clair Field
RONA RIDGE
WEST SHETLAND PLATFORM
ORKNEY-SHETLAND PLATFORM
Walls Boudary Fault
S
WEST ORKNEY BASIN
O
Fig.2
DH
ORCADIAN BASIN
NHT
NORTH MINCH BASIN
MORAY FIRTH BASIN
Helmsdale Fault
Great Glen Fault
Moine Thrust
CHT
a

Figure 2

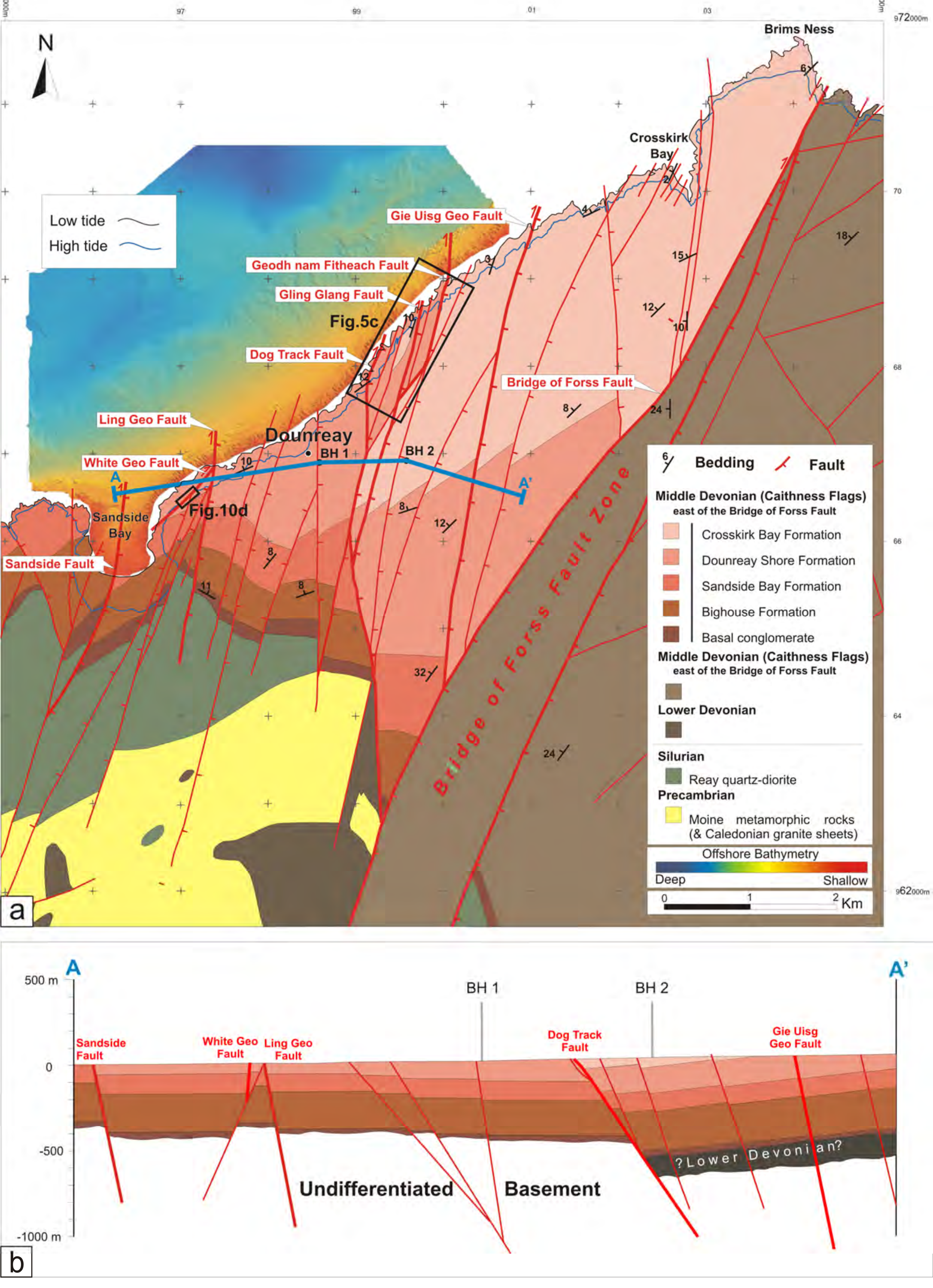
N
Low tide
High tide
Brims Ness
Crosskirk Bay
Gie Uisg Geo Fault
Geodh nam Fitheach Fault
Gling Glang Fault
Fig.5c
Dog Track Fault
Bridge of Forss Fault
Ling Geo Fault
Dounreay
BH 1
BH 2
White Geo Fault
A
A'
Fig.10d
Sandside Bay
Sandside Fault
Bridge of Forss Fault Zone
Bedding
Fault
Middle Devonian (Caithness Flags)
east of the Bridge of Forss Fault
Crosskirk Bay Formation
Dounreay Shore Formation
Sandside Bay Formation
Bighouse Formation
Basal conglomerate
Middle Devonian (Caithness Flags)
east of the Bridge of Forss Fault
Lower Devonian
Silurian
Reay quartz-diorite
Precambrian
Moine metamorphic rocks
(& Caledonian granite sheets)
Offshore Bathymetry
Deep
Shallow
0 1 2 Km
a
500 m
0
-500
-1000 m
Sandside Fault
White Geo Fault
Ling Geo Fault
Dog Track Fault
Gie Uisg Geo Fault
?Lower Devonian?
Undifferentiated Basement
b

Figure 3

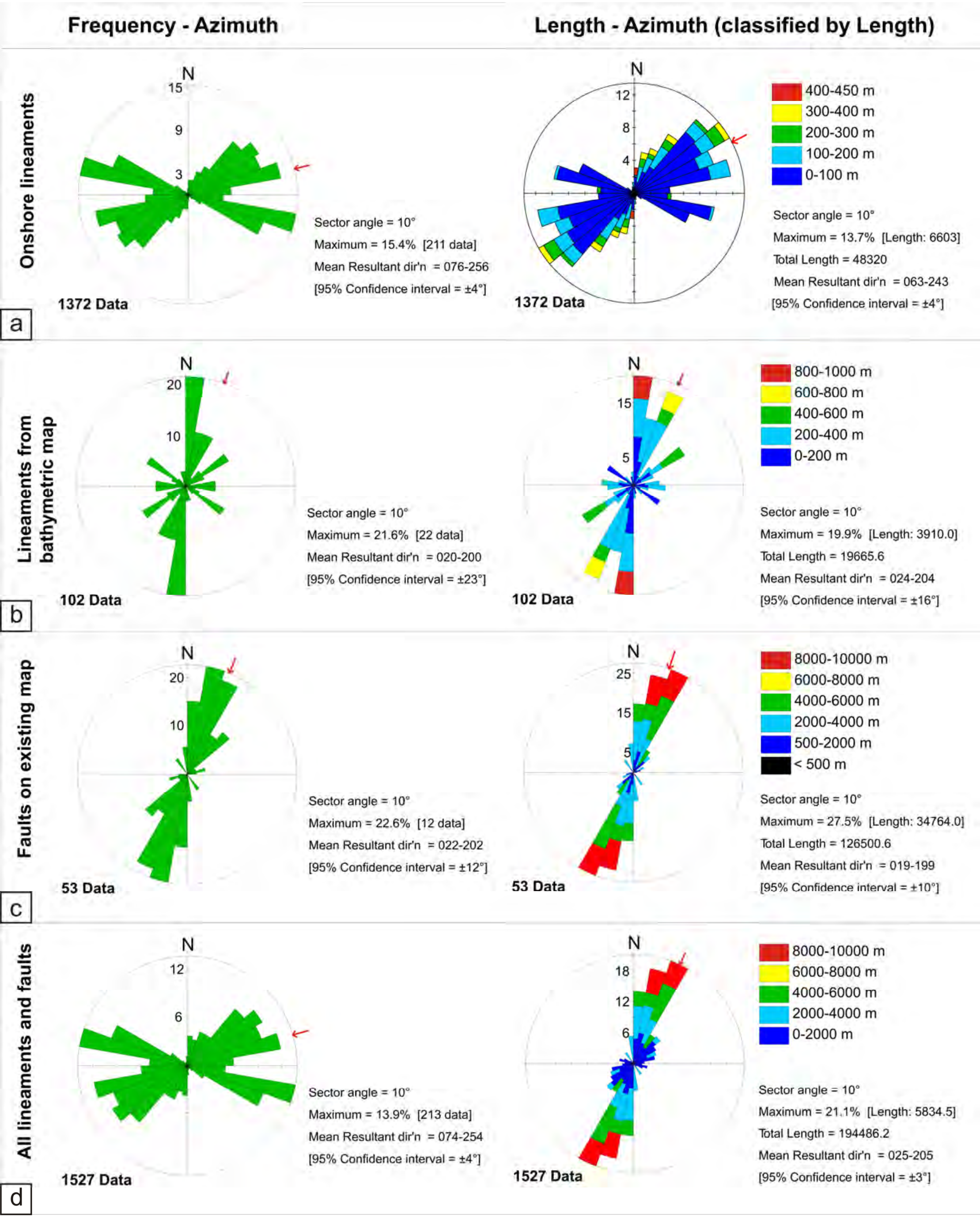
Frequency - Azimuth
Length - Azimuth (classified by Length)
Onshore lineaments
N
15
9
3
Sector angle = 10°
Maximum = 15.4% [211 data]
Mean Resultant dir'n = 076-256
[95% Confidence interval = ±4°]
1372 Data
N
12
8
4
400-450 m
300-400 m
200-300 m
100-200 m
0-100 m
Sector angle = 10°
Maximum = 13.7% [Length: 6603]
Total Length = 48320
Mean Resultant dir'n = 063-243
[95% Confidence interval = ±4°]
1372 Data
a
Lineaments from bathymetric map
N
20
10
Sector angle = 10°
Maximum = 21.6% [22 data]
Mean Resultant dir'n = 020-200
[95% Confidence interval = ±23°]
102 Data
N
15
5
800-1000 m
600-800 m
400-600 m
200-400 m
0-200 m
Sector angle = 10°
Maximum = 19.9% [Length: 3910.0]
Total Length = 19665.6
Mean Resultant dir'n = 024-204
[95% Confidence interval = ±16°]
102 Data
b
Faults on existing map
N
20
10
Sector angle = 10°
Maximum = 22.6% [12 data]
Mean Resultant dir'n = 022-202
[95% Confidence interval = ±12°]
53 Data
N
25
15
5
8000-10000 m
6000-8000 m
4000-6000 m
2000-4000 m
500-2000 m
< 500 m
Sector angle = 10°
Maximum = 27.5% [Length: 34764.0]
Total Length = 126500.6
Mean Resultant dir'n = 019-199
[95% Confidence interval = ±10°]
53 Data
c
All lineaments and faults
N
12
6
Sector angle = 10°
Maximum = 13.9% [213 data]
Mean Resultant dir'n = 074-254
[95% Confidence interval = ±4°]
1527 Data
N
18
12
6
8000-10000 m
6000-8000 m
4000-6000 m
2000-4000 m
0-2000 m
Sector angle = 10°
Maximum = 21.1% [Length: 5834.5]
Total Length = 194486.2
Mean Resultant dir'n = 025-205
[95% Confidence interval = ±3°]
1527 Data
d

Figure 4 Click here to download Figure Fig4.pdf

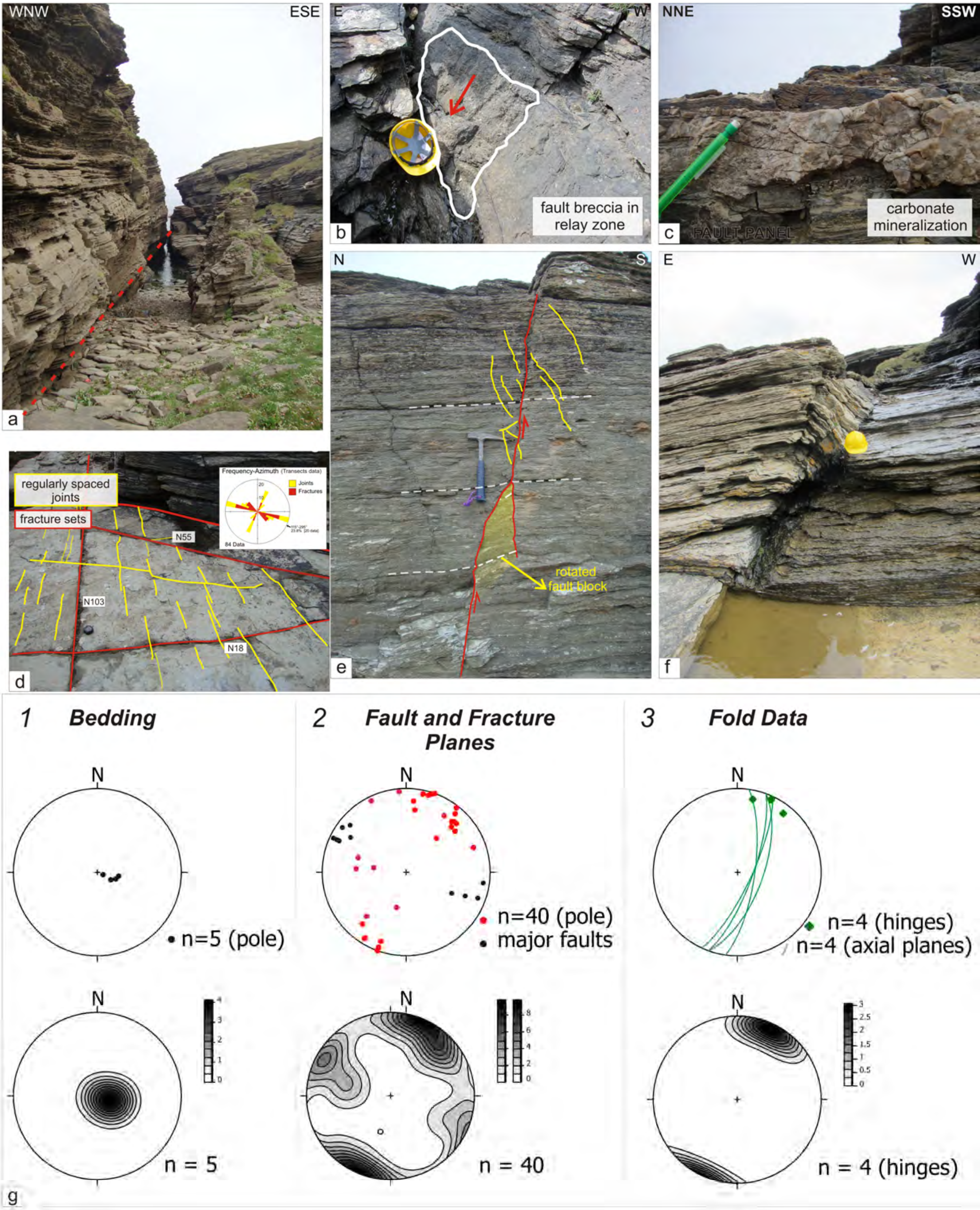

Figure 5

Click here to download Figure Fig5.pdf

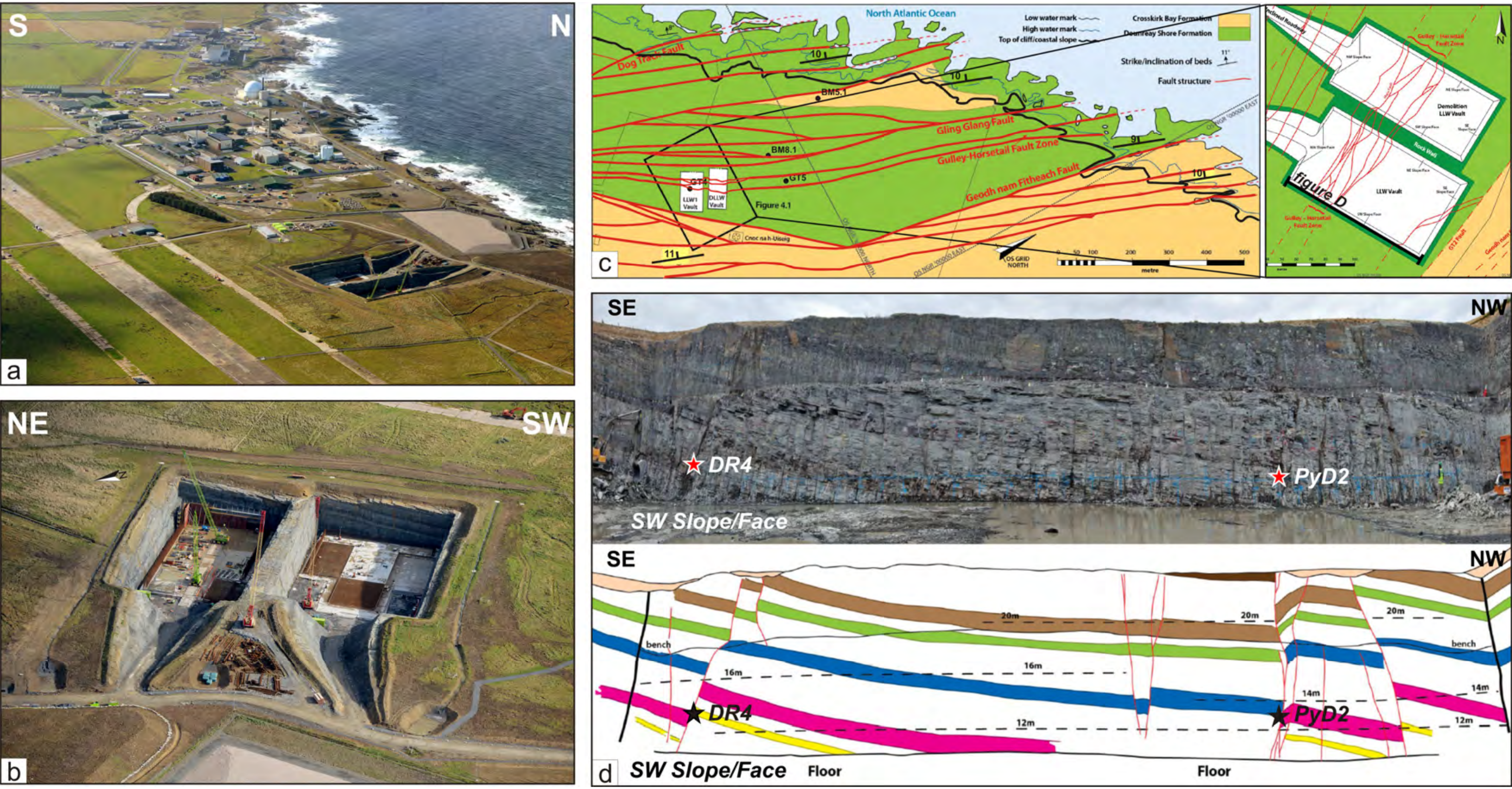

Figure 6

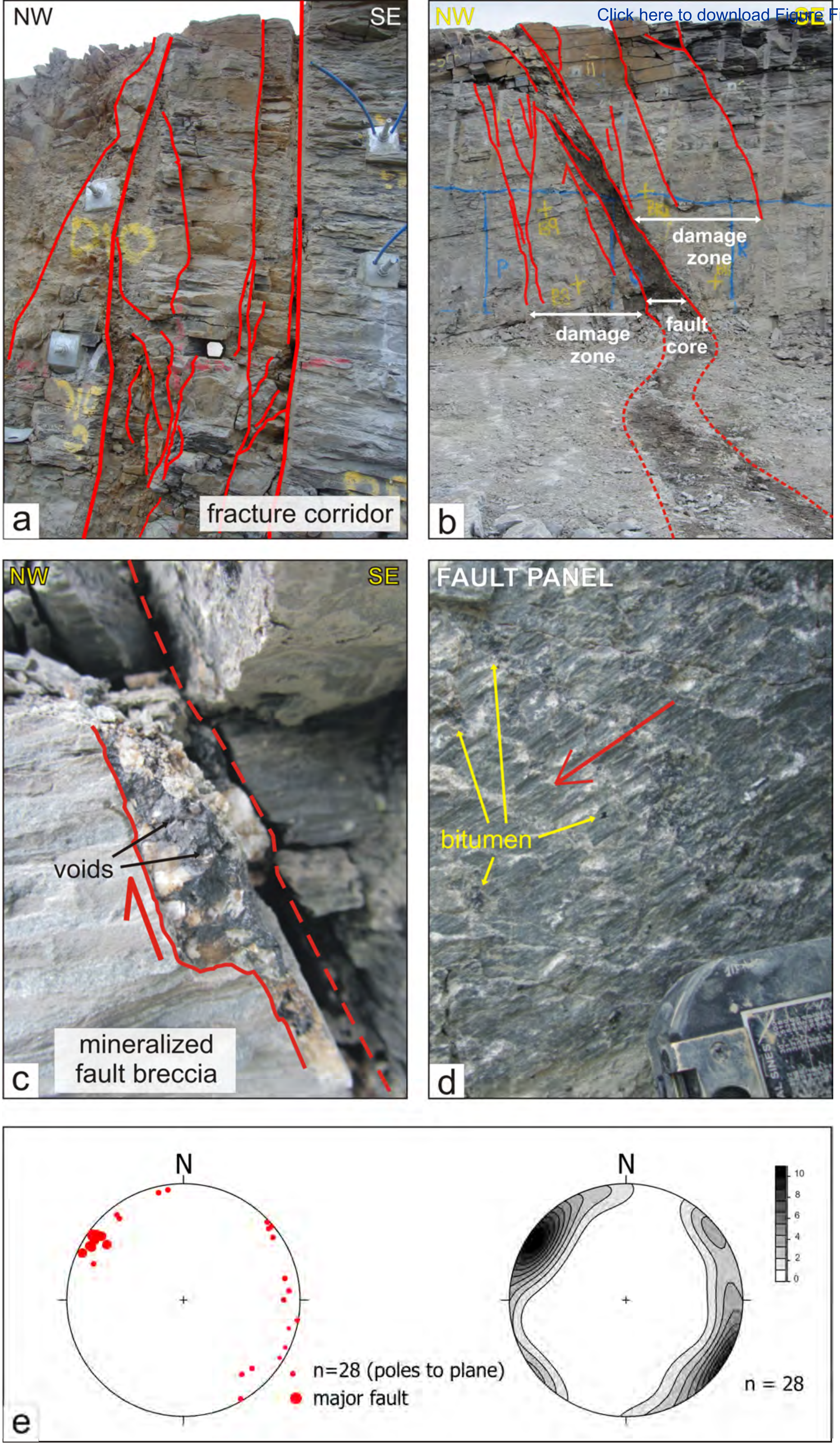

NW
SE
fracture corridor
a
NW
SE
damage zone
damage zone
fault core
b
NW
SE
voids
mineralized fault breccia
c
FAULT PANEL
bitumen
d
N
n=28 (poles to plane)
major fault
N
10
8
6
4
2
0
n = 28
e

Figure 7

Click here to download Figure Fig7.pdf

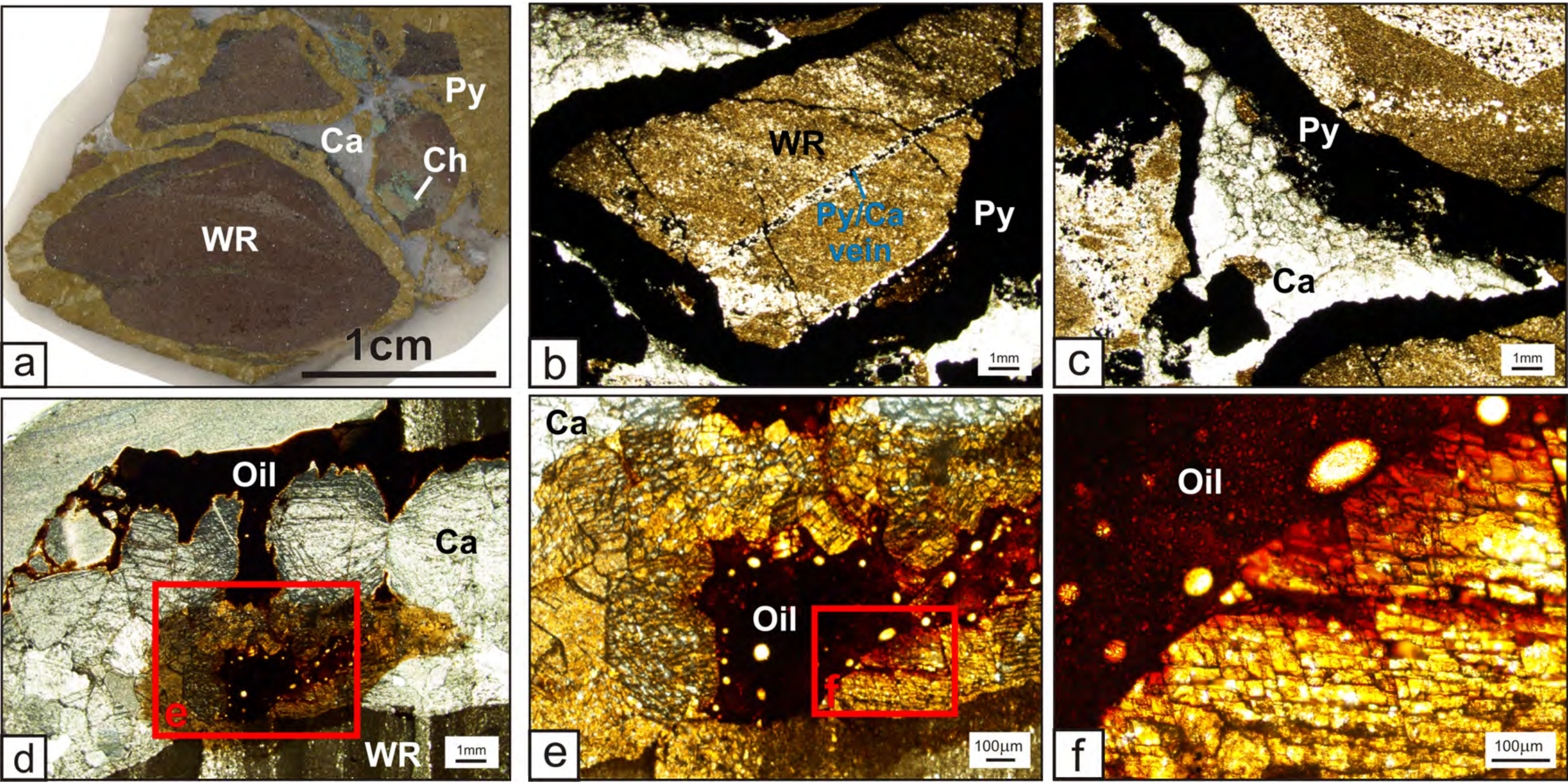

Figure 8

Click here to download Figure Fig8.pdf

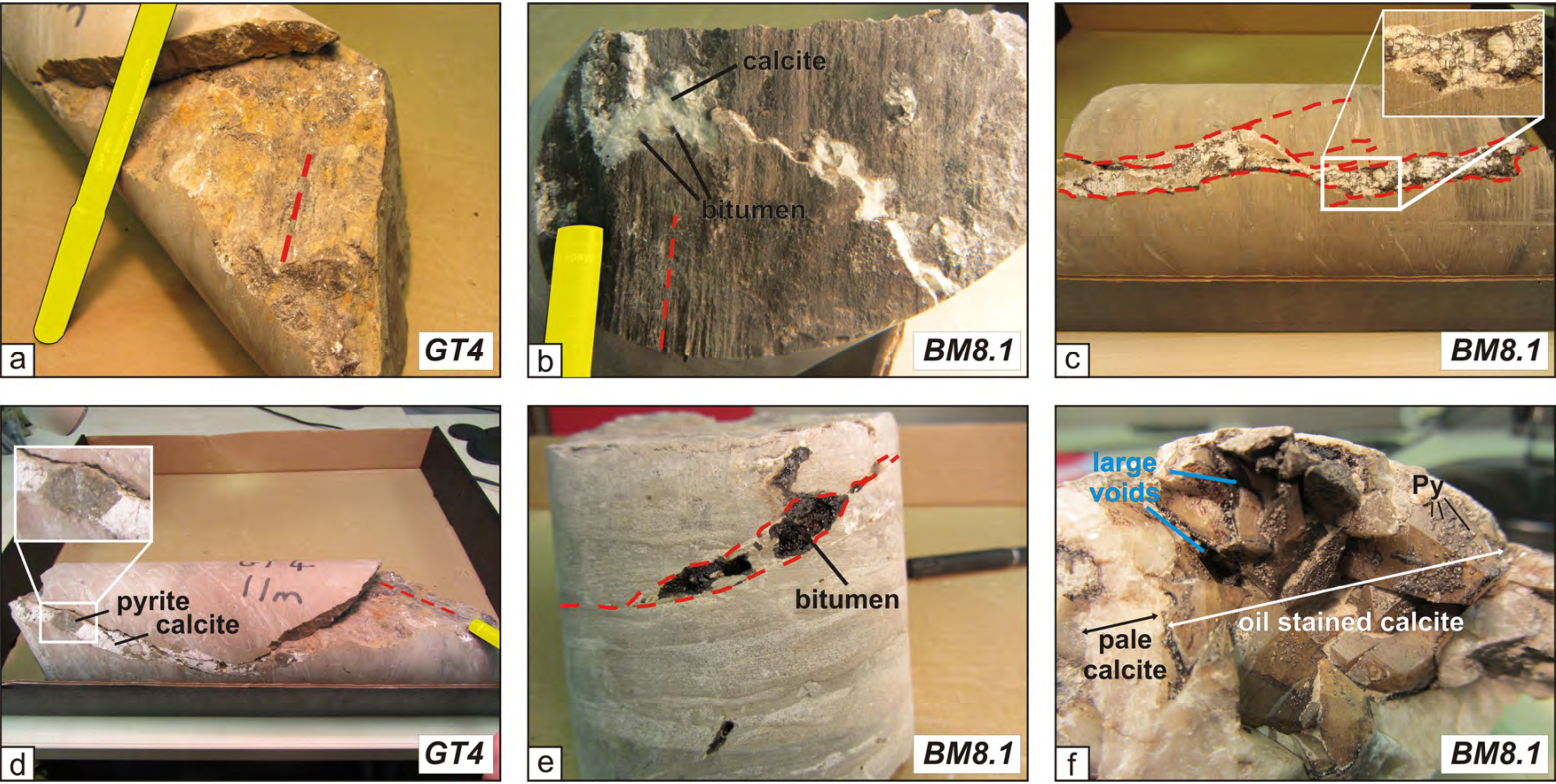

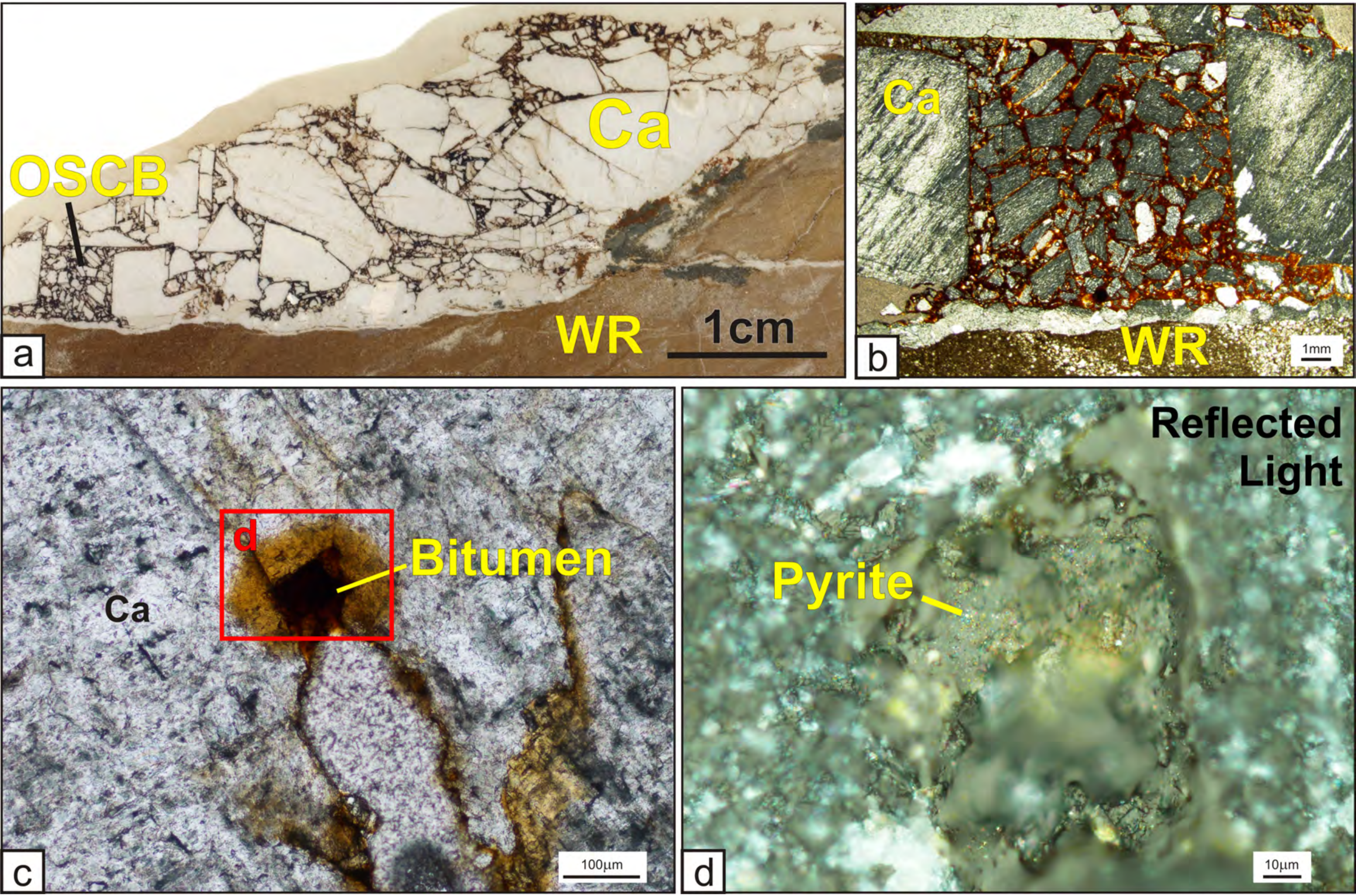
a
OSCB
Ca
WR
1cm
b
Ca
WR
1mm
c
d
Bitumen
Ca
100µm
d
Reflected Light
Pyrite
10µm

Figure 10

Click here to download Figure Fig10.pdf

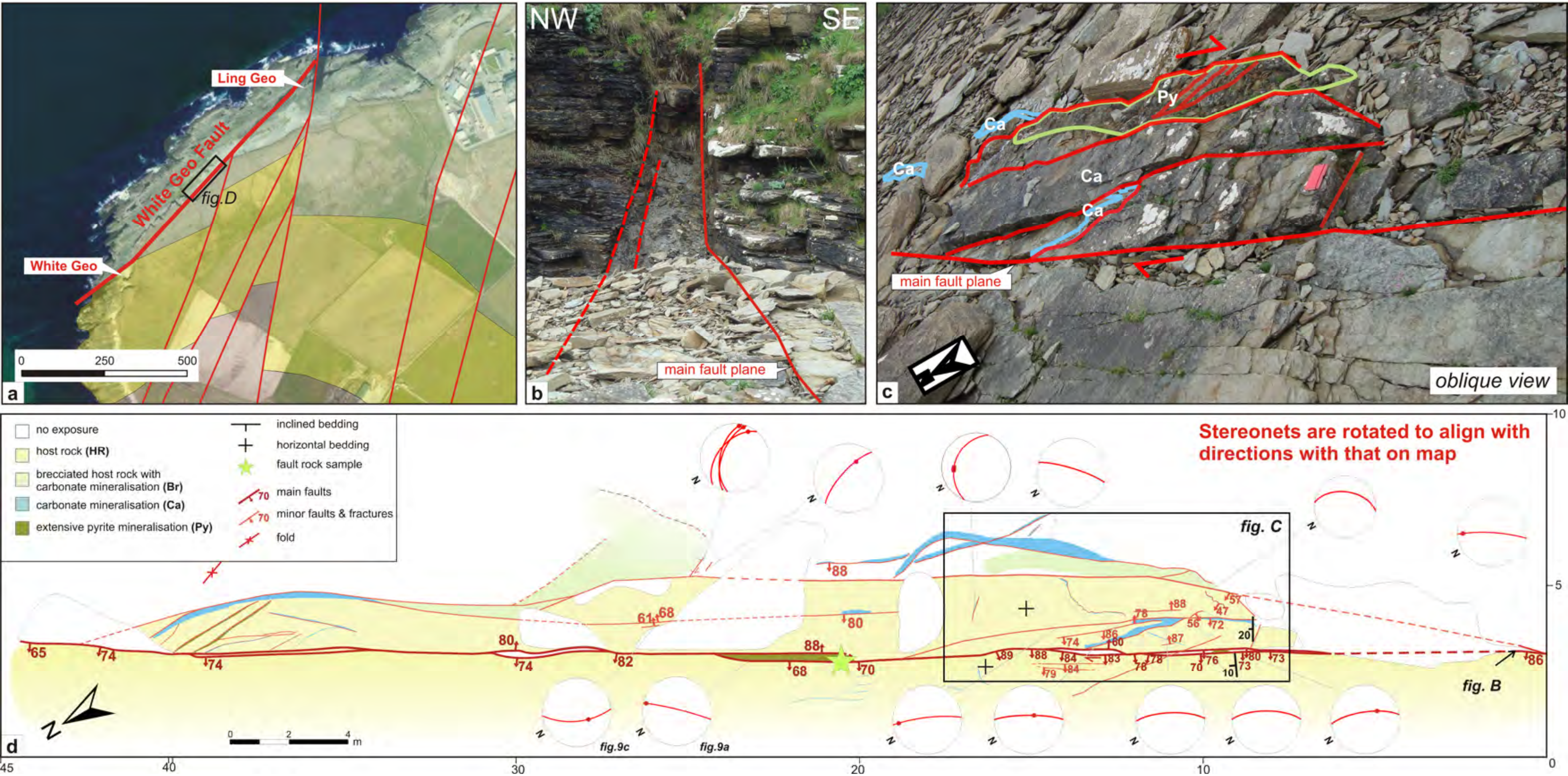

Figure 11

Click here to download Figure Fig11.pdf

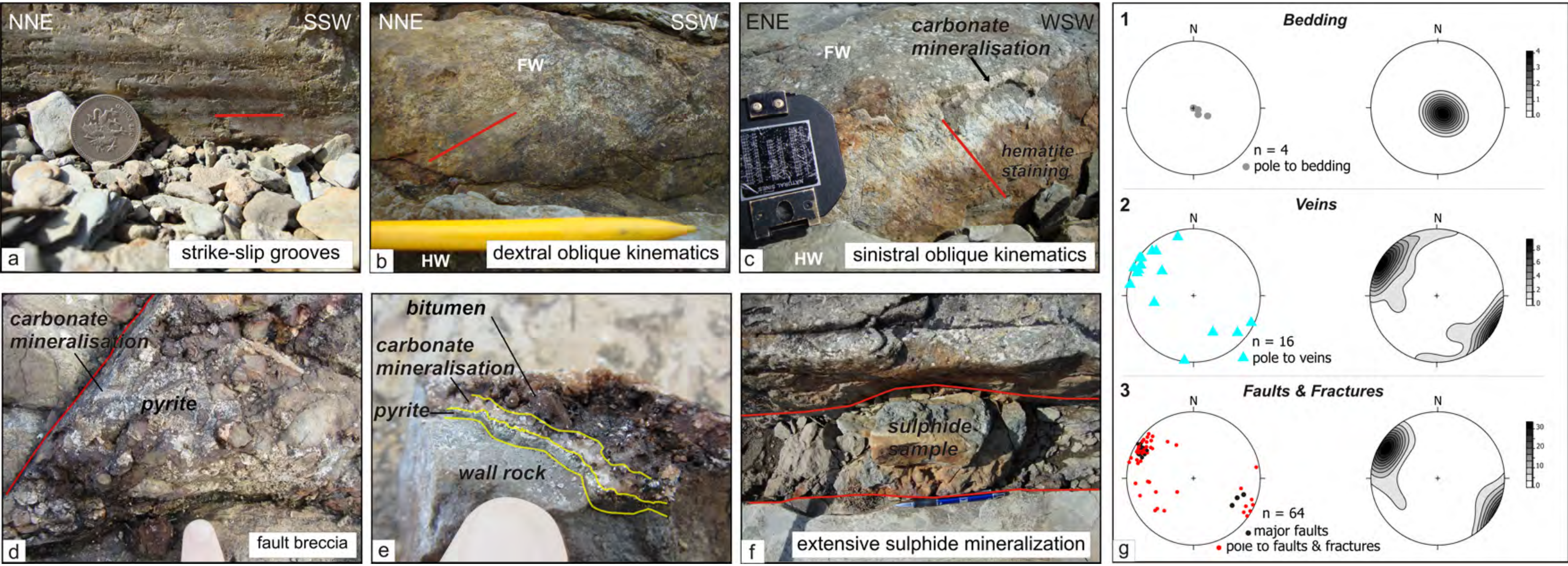

Figure 12

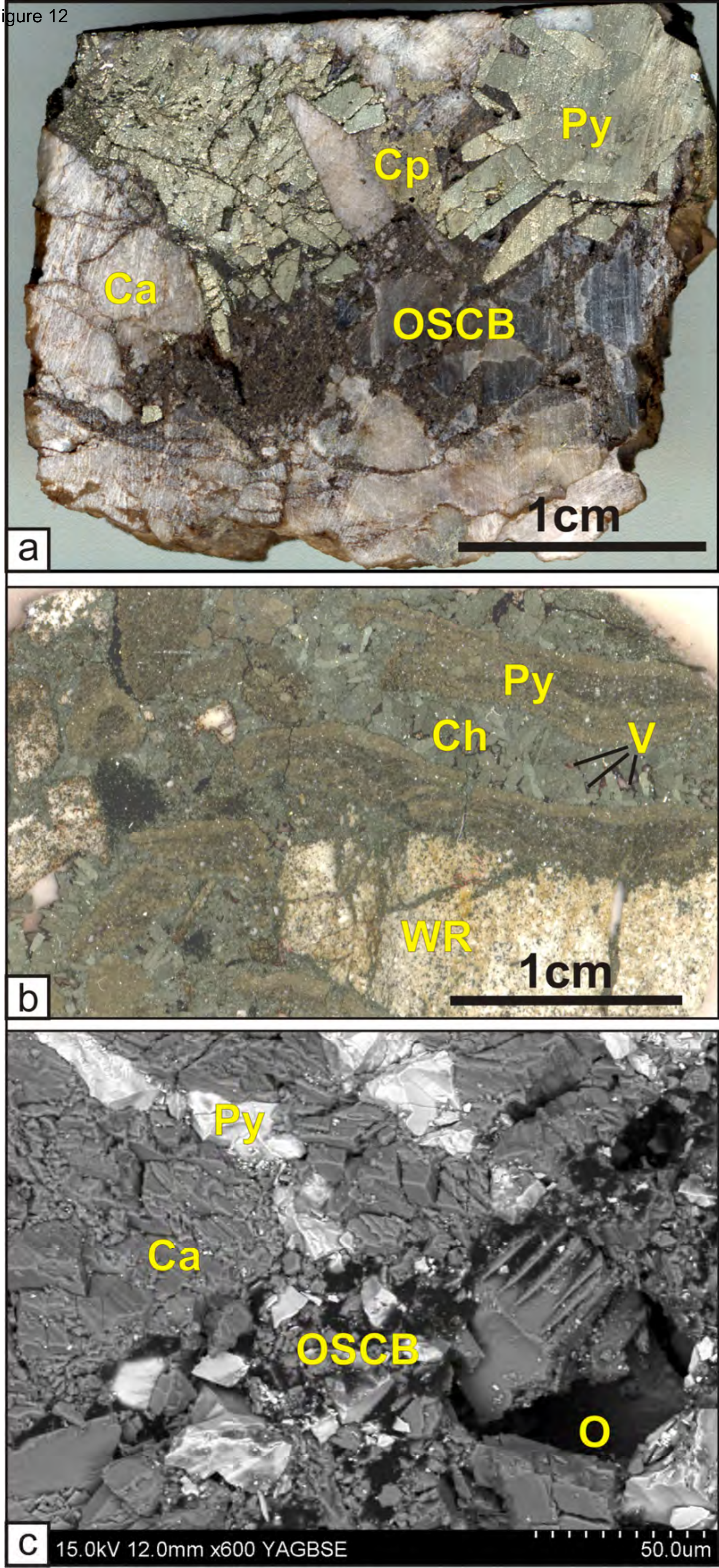

Py = Pyrite
Ca = Calcite
CP = Chalcopyrite
OSCB = Oil Stained Calcite Breccia

Py = Pyrite
WR = Wallrock
Ch = Chalcocite
V = Vugs

Py = Pyrite
Ca = Calcite
O = Oil
OSCB = Oil Stained Calcite Breccia

Figure 13

Click here to download Figure Fig 13.pdf

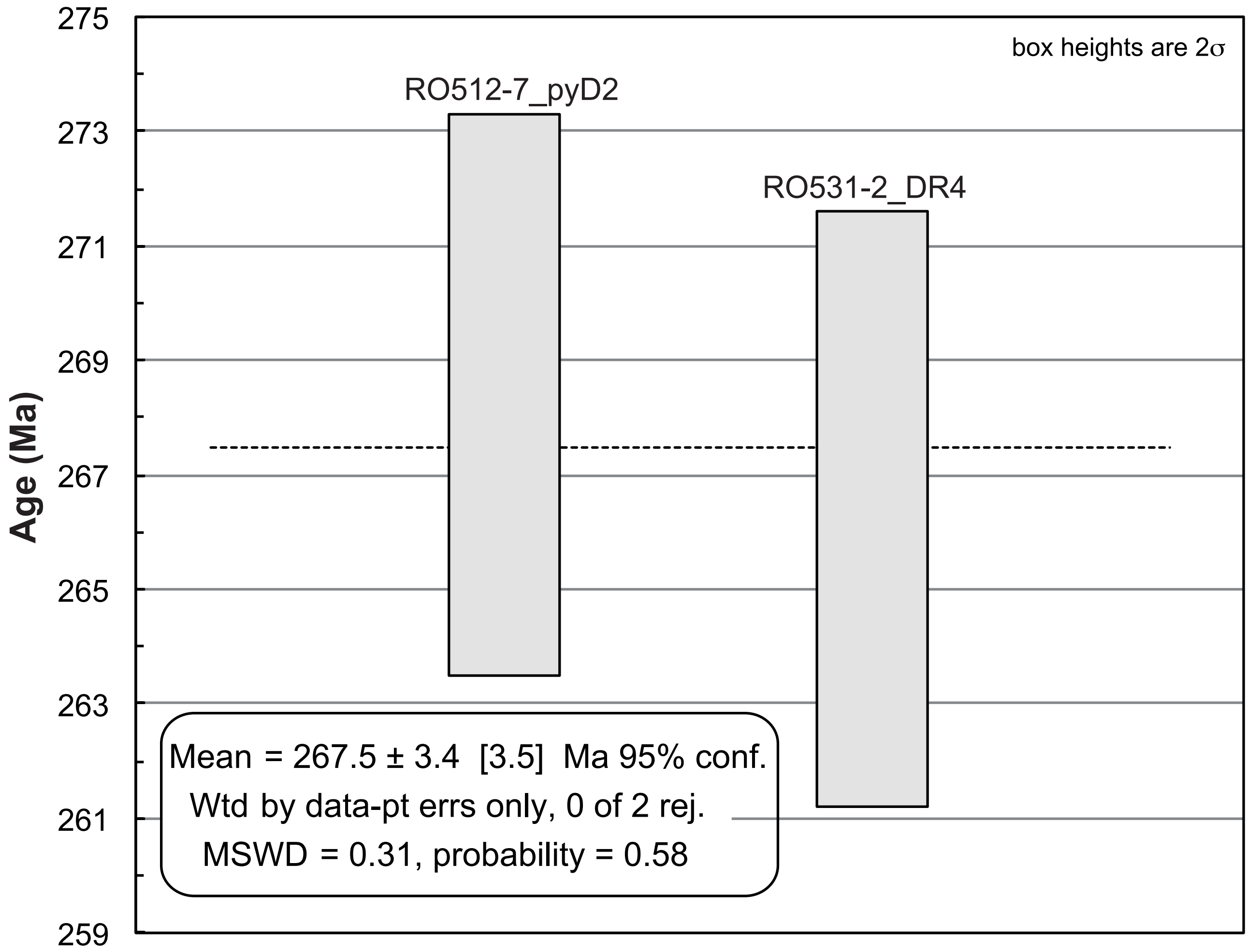

Figure 14

Click here to download Figure Fig14.pdf

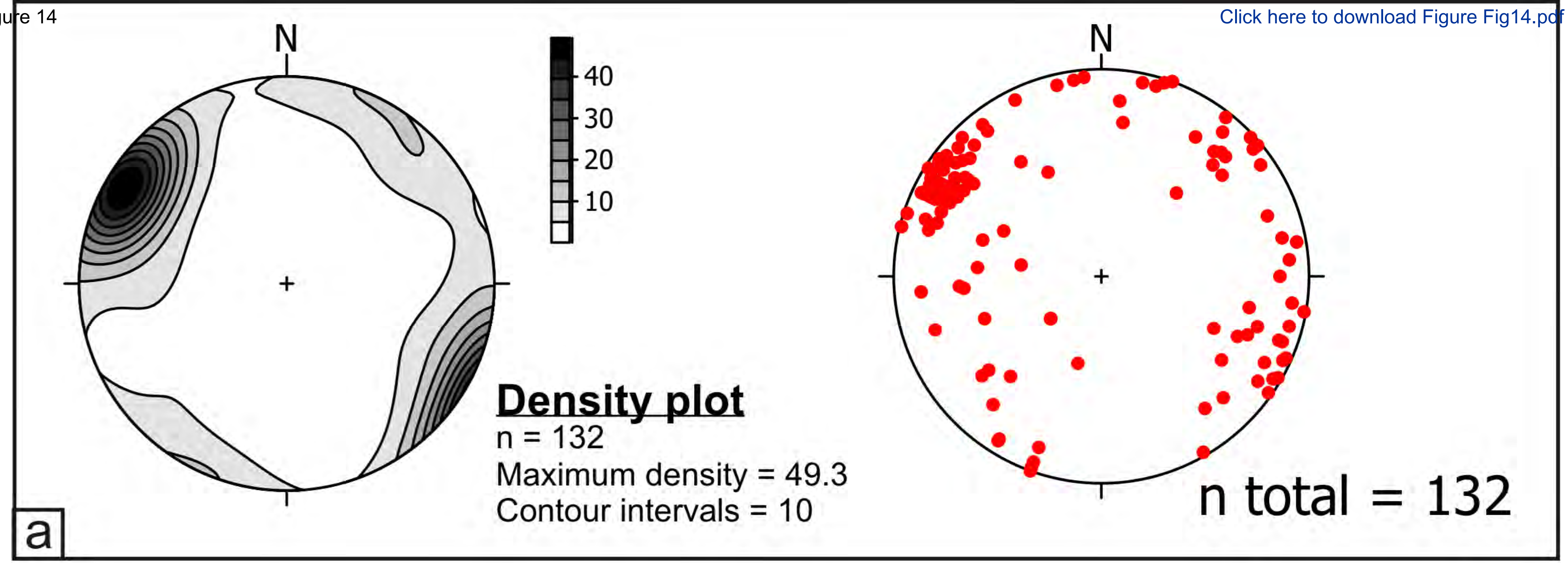

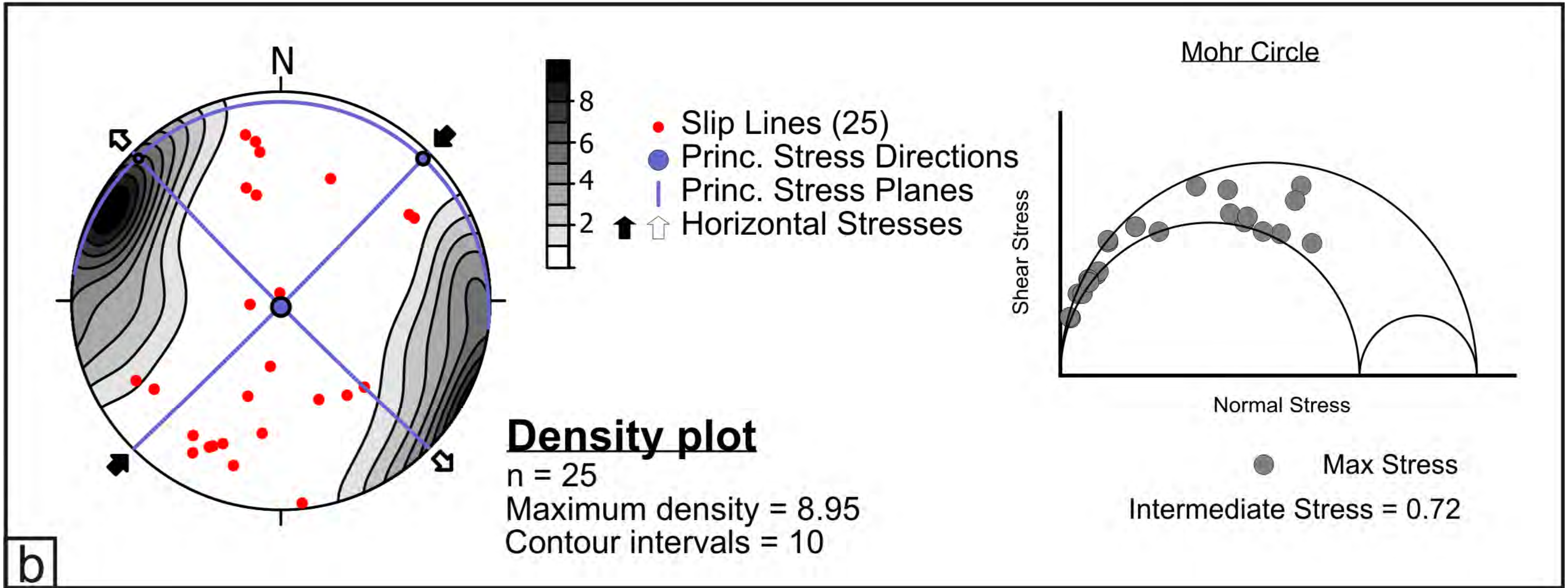

Figure 15

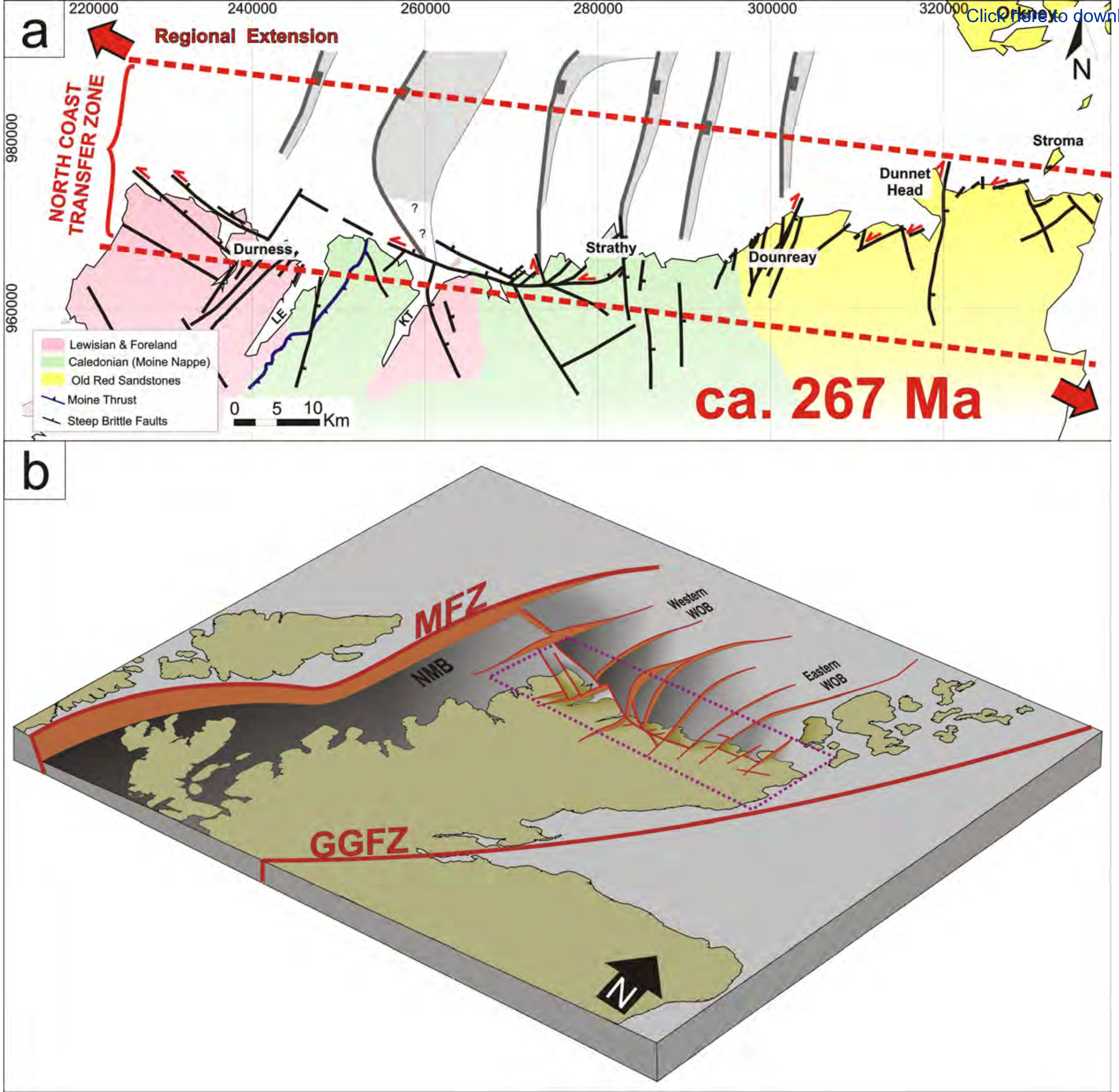

a
220000
240000
260000
280000
300000
320000
980000
960000
Regional Extension
NORTH COAST TRANSFER ZONE
N
Orkney
Stroma
Dunnet Head
Durness
Strathy
Dounreay
LE
KT
Lewisian & Foreland
Caledonian (Moine Nappe)
Old Red Sandstones
Moine Thrust
Steep Brittle Faults
0 5 10 Km
ca. 267 Ma
b
MFZ
NMB
Western WOB
Eastern WOB
GGFZ
N